

# STABILIZATION OF THE NONCONFORMING VIRTUAL ELEMENT METHOD

S. BERTOLUZZA\*, G. MANZINI, M. PENNACCHIO, AND D. PRADA

**ABSTRACT.** We address the issue of designing robust stabilization terms for the nonconforming virtual element method. To this end, we transfer the problem of defining the stabilizing bilinear form from the elemental nonconforming virtual element space, whose functions are not known in closed form, to the dual space spanned by the known functionals providing the degrees of freedom. By this approach, we manage to construct different bilinear forms yielding optimal or quasi-optimal stability bounds and error estimates, under weaker assumptions on the tessellation than the ones usually considered in this framework. In particular, we prove optimality under geometrical assumptions allowing a mesh to have a very large number of arbitrarily small edges per element. Finally, we numerically assess the performance of the VEM for several different stabilizations fitting with our new framework on a set of representative test cases.

## 1. INTRODUCTION

Solving partial differential equations on polygonal and polyhedral meshes has become a major issue in the last decades, and a number of numerical methods have been proposed to this end in the technical literature. Many of these methods are based on some kind of generalization of the finite element method (FEM) and must address the critical issue that the construction of shape functions on elements with arbitrary geometric shapes is a very difficult task. The virtual element method (VEM), originally proposed in [8] for the Poisson equation and then extended to convection-reaction-diffusion problems with variable coefficients in [9], brilliantly overcomes this issue. The method was designed from the very beginning to work on generally shaped elements with high order of accuracy, and does not require an explicit knowledge of the basis functions that generate the finite element approximation space. Indeed, the formulation of the method and its practical implementations are based on suitable polynomial projections that are always computable from a careful choice of the degrees of freedom. Optimal numerical approximations of arbitrary order and arbitrary regularity to PDE solutions are possible in two and three dimensions using very general mesh families, including meshes that are often considered as pathological in other methods. VEM is intimately connected with other finite element approaches: the connection between the VEM and finite elements on polygonal/polyhedral meshes is thoroughly investigated in [34, 45, 55], between VEM and discontinuous skeletal gradient discretizations in [45], and between the VEM and the BEM-based FEM method in [33].

The conforming VEM was originally developed as a variational reformulation of the *nodal* mimetic finite difference (MFD) method [11, 29, 54] for solving diffusion problems on unstructured polygonal meshes. The issue of its efficient implementation is considered in several papers (cf. [6, 21, 22, 30, 42, 43]). A survey on the MFD method can be found in the review paper [53] and the research

---

*Key words and phrases.* Virtual element method, nonconforming Galerkin method, polygonal mesh, stabilization, dual norms .

\* Corresponding author.

monograph [12]. The scheme inherits the flexibility of the MFD method with respect to the admissible meshes and this feature is well reflected in the many significant applications that have been developed so far, see, for example, [3, 5, 9, 10, 14–16, 18, 31, 37, 38, 41, 46, 59–61, 63].

The nonconforming virtual element method was originally proposed in [7] for the solution of the Poisson equation. Then, it was extended to general elliptic equations [17, 35], fractional reaction-subdiffusion equations [52], eigenvalue problems [48], Helmholtz equations [56–58], Stokes, Darcy-Stokes and Navier-Stokes equations [32, 67, 68], elasticity problems [64], nonconforming anisotropic estimates [36], plate bending problems, biharmonic equation, highly-order elliptic equations [4, 51, 65, 66].

The nonconforming virtual element method possesses several interesting features. First, the VEM admits meshes whose elements are polygons (2D) and polyhedra (3D) with, in principle, almost arbitrary geometric shapes. This flexibility in the mesh choice may have a significant impact in both numerical approximation and mesh generation. Second, we can construct stable virtual element methods in a straightforward way for any polynomial degree. Moreover, such construction can be readily generalized from two to three space dimensions, and, in principle, to any space dimensions. Third, the formulation and implementation of the nonconforming VEM needs less degrees of freedom than other methods, such as, for example discontinuous Galerkin. Note also that unknowns associated with the interior of the mesh elements can be eliminated by static condensation. This feature makes the VEM competitive in terms of computational efficiency with respect to other discretization methods.

As it happens in the conforming VEM, the stability and convergence of the nonconforming VEM rely on the fundamental properties of *consistency* and *stability*. Consistency is an exactness property that states that the approximated bilinear forms of the discrete variational formulation are exact on the subspace of polynomials locally defined in each element. In turn, stability follows from a suitable *stabilization term*, whose role is to control the non polynomial component of the discretization. When the polygonal elements satisfy a quite restrictive shape regularity condition, basically equivalent to requiring that they can be decomposed into a (small) number of shape regular triangles, we know that the euclidean product of the degrees of freedom of the virtual element functions is an effective stabilization term and provides optimal results. However, greater care must be taken in designing the stabilization term when we consider more general elements, such as, for instance, elements with very small edges.

In the conforming case, the design of computable stabilization terms yielding optimal results relies on the fact that we can compute the trace of the virtual element functions on the elemental boundaries from the degrees of freedom. Conversely, in the nonconforming case, the knowledge of the degrees of freedom does not allow us to retrieve the trace of the corresponding functions without solving a partial differential equation in the element. In the VEM terminology, we say that the trace on the elemental boundary of a nonconforming virtual function is “*noncomputable*”. On the positive side, the functionals yielding the degrees of freedom in a polygonal element  $P$  span a known subspace  $V_k^*(P)$  of the dual space  $(H^1(P))'$ . Such a space satisfies a uniformly stable duality relation with the local VEM space  $V_k^h(P)$ . This property, which is inherent to the nonconforming nature of the approximation space and does not hold for the conforming VEM, allows us to reduce the problem of designing the stabilization bilinear form on the non conforming VEM space  $V_k^h(P)$ , to the design of a semi-inner product in  $V_k^*(P)$ , yielding a suitable seminorm for  $(H^1(P))'$ . We can then consider and analyze different strategies for the construction of such semi-inner product,

yielding optimal or quasi-optimal stability and convergence results under weaker assumptions on the polygonal tessellation.

We conclude this introductory section with a review of some basic definitions about the functional setting and the notation that we use in the paper. The rest of the paper is organized as follows. In Section 2 we introduce the model problem and its discretization by the nonconforming virtual element approximation. In Section 3 we present an abstract theoretical framework for the algebraic construction of the semi-inner products in finite dimensional dual spaces. In Section 4 and 5 we discuss the construction of the stabilization terms for the nonconforming VEM in such a framework. In Section 6 we investigate the performance of the method on a set of suitable numerical experiments. In Section 7 we offer our final remarks and conclusions.

**1.1. Basic definitions, notation and functional setting.** Let the computational domain  $\Omega$  be an open, bounded, connected subset of  $\mathbb{R}^2$  with polygonal boundary  $\Gamma$ . We consider a family of domain partitionings  $\mathcal{T} = \{\Omega_h\}_{h \in \mathcal{H}}$ . Every partition  $\Omega_h$ , the *mesh*, is a finite collection of non overlapping polygonal elements  $P$ , which are such that  $\overline{\Omega} = \cup_{P \in \Omega_h} \overline{P}$ . Further assumptions on the mesh family  $\mathcal{T}$  and the meshes  $\Omega_h$  will be detailed in Section 4.

For  $P \in \Omega_h$ , we denote the boundary of  $P$  by  $\partial P$ , its diameter by  $h_P = \max_{\mathbf{x}, \mathbf{y} \in P} |\mathbf{x} - \mathbf{y}|$ , its area by  $|P|$ , and the outward unit normal to the boundary by  $\mathbf{n}_P$ . Each elemental boundary  $\partial P$  is formed by a sequence of one-dimensional non-intersecting straight edges  $e$  with lenght  $h_e$ . The symbols  $\mathcal{E}_P$ ,  $\mathcal{E}_\Gamma$  and  $\mathcal{E}$  respectively denote the set of edges that form the boundary of the element  $P$ , the set of mesh edges on the boundary  $\Gamma$ , and the set of all the mesh edges.

We use standard definitions and notations for Sobolev spaces, and for the corresponding norms and seminorms, cf. [1]. More precisely, let  $\omega$  be a  $d$ -dimensional domain,  $d = 1, 2$ . We let  $L^2(\omega)$  denote the Hilbert functional space of the real-valued, square integrable functions defined on  $\omega$ , and  $H^m(\omega)$  the Sobolev functional space of the real-valued functions in  $L^2(\omega)$  whose weak derivatives up to the order  $m$  are also in  $L^2(\omega)$ . We let  $\|\cdot\|_{0,\omega}$  denote the standard norm in  $L^2(\omega)$ , and  $\|\cdot\|_{m,\omega}$  and  $|\cdot|_{m,\omega}$  denote respectively the standard norm and seminorm in  $H^m(\omega)$ . On the elemental boundary  $\partial P$ , we also consider the functional space

$$H^{\frac{1}{2}}(\partial P) = \left\{ v \in L^2(\partial P) \text{ such that } \|v\|_{0,\partial P} + |v|_{1/2,\partial P} < \infty \right\}, \quad (1)$$

and its dual  $H^{-\frac{1}{2}}(\partial P)$ . In (1),  $| \cdot |_{1/2,\partial P}$  is the seminorm defined by

$$|v|_{1/2,\partial P}^2 = \int_{\partial P \times \partial P} \frac{|v(x) - v(y)|^2}{|x - y|^2} dx dy. \quad (2)$$

We recall that the trace  $v|_{\partial P}$  of a function  $v \in H^1(P)$  belongs to  $H^{\frac{1}{2}}(\partial P)$ . Similar definitions hold for  $H^{\frac{1}{2}}(e)$ ,  $H^{-\frac{1}{2}}(e)$ ,  $H^{\frac{1}{2}}(\Gamma)$ ,  $H^{-\frac{1}{2}}(\Gamma)$ , and for the corresponding norms and seminorms.

For a given nonnegative integer  $\ell$ , we let  $\mathbb{P}_\ell(\omega)$  denote the space of polynomials of degree up to  $\ell$  defined on  $\omega$ , and we conventionally define  $\mathbb{P}_{-1}(\omega) = \{0\}$ . Furthermore,  $\mathbb{P}_\ell(\Omega_h)$  denotes the space of discontinuous bivariate polynomials of degree up to  $\ell$  defined on the elements of  $\Omega_h$ :

$$\mathbb{P}_\ell(\Omega_h) = \left\{ p \in L^2(\Omega) : p|_P \in \mathbb{P}_\ell(P) \ \forall P \in \Omega_h \right\}.$$

We let  $\mathcal{M}_\ell(\omega)$  denote the set of scaled monomials on  $\omega$  of degree up to  $\ell$ , given by

$$\mathcal{M}_\ell(\omega) = \left\{ m_\alpha(\mathbf{x}) = \left( \frac{\mathbf{x} - \mathbf{x}_\omega}{h_\omega} \right)^\alpha, \quad \alpha \in \mathbb{N}^d \text{ with } |\alpha| \leq \ell \right\},$$

where  $\mathbf{x}_\omega$  denotes the center of mass of  $\omega$  and  $h_\omega$  its diameter. The set  $\mathcal{M}_\ell(\omega)$  forms a basis for the space  $\mathbb{P}_\ell(\omega)$ .

On  $\Omega_h$  and for every integer  $m > 0$ , we consider the broken Sobolev space

$$H^m(\Omega_h) = \left\{ v \in L^2(\Omega) : v|_P \in H^m(P) \text{ for all } P \in \Omega_h \right\},$$

endowed with the broken Sobolev norm and seminorm

$$\|v\|_{m,h}^2 = \sum_{P \in \Omega_h} \|v\|_{m,P}^2, \quad |v|_{m,h}^2 = \sum_{P \in \Omega_h} |v|_{m,P}^2 \quad \forall v \in H^m(\Omega_h). \quad (3)$$

Let  $e \in \mathcal{E}_{P+} \cap \mathcal{E}_{P-}$  be an internal edge shared by the polygonal elements  $P^+$  and  $P^-$ , and  $v$  a function of  $H^1(\Omega_h)$ . We denote the traces of  $v$  on  $e$  from inside the elements  $P^\pm$  by  $v_e^\pm$ , and the unit normal vectors to  $e$  pointing from  $P^\pm$  to  $P^\mp$  by  $\mathbf{n}_e^\pm$ . Then, we introduce the *jump operator*, which is defined as

$$[\![v]\!] = \begin{cases} v_e^+ \mathbf{n}_e^+ + v_e^- \mathbf{n}_e^- & \text{for every internal edge } e \in \mathcal{E}_{P+} \cap \mathcal{E}_{P-}, \\ v_e \mathbf{n}_e & \text{for every boundary edge } e \in \mathcal{E}_\Gamma. \end{cases}$$

The normal vectors to the edges on the domain boundary  $\Gamma$  are pointing out of  $\Omega$ .

For any positive integer  $k$ , the nonconforming space  $H_k^{1,nc}(\Omega_h)$  is the subspace of the broken Sobolev space  $H^1(\Omega_h)$  defined as

$$H_k^{1,nc}(\Omega_h) = \left\{ v \in H^1(\Omega_h) : \int_e [\![v]\!] \cdot \mathbf{n}_e q = 0 \quad \forall q \in \mathbb{P}_{k-1}(e), \quad \forall e \in \mathcal{E} \right\}. \quad (4)$$

The nonconforming space with  $k = 1$  has the minimal regularity that is required in the formulation of the VEM, see Section 2, and for the convergence analysis, see Reference [7].

For the discontinuous functions of  $H^1(\Omega_h)$ ,  $|\cdot|_{1,h}$  is only a seminorm. However, it becomes a norm on the nonconforming space  $H_k^{1,nc}(\Omega_h)$  since the Poincaré-Friedrichs type inequality  $\|v\|_0^2 \leq C|v|_{1,h}^2$  holds for every  $v \in H_k^{1,nc}(\Omega_h)$ ,  $k \geq 1$ . Here,  $C$  is a real, positive constant independent of  $h$ , cf. [27]; see also [23, Lemma 2.6], which can be leveraged to obtain such a bound under weaker conditions on the mesh.

We introduce the elliptic projection operator  $\Pi_k^{\nabla,P} : H^1(P) \rightarrow \mathbb{P}_k(P)$ , defined as follows: for every  $v \in H^1(P)$ , the  $k$ -degree polynomial  $\Pi_k^{\nabla,P} v$  is the solution of the variational problem:

$$\int_P \nabla \left( \Pi_k^{\nabla,P} v - v \right) \cdot \nabla q = 0 \quad \forall q \in \mathbb{P}_k(P),$$

with the additional condition

$$\int_{\partial P} \left( \Pi_k^{\nabla,P} v - v \right) = 0, \quad (5)$$

which handles the kernel of the gradient operator. We note that  $\Pi_k^{\nabla,P}$  is a polynomial-preserving operator, i.e.,  $\Pi_k^{\nabla,P} q = q$  for every polynomial function  $q \in \mathbb{P}_k(P)$ .

Finally, throughout the paper we use the notation  $v \simeq w$ ,  $v \lesssim w$  and  $v \gtrsim w$  to indicate that there are suitable positive, real constants  $c_*$  and  $c^*$  such that  $c_*v \leq w \leq c^*v$ ,  $v \leq c^*w$  and  $v \geq c^*w$ . These constants are independent of the mesh size  $h$  but may depend on other discretization parameters such as the mesh regularity constants and the polynomial order of the method. The constants  $c_*$  and  $c^*$ , and the generic constant  $C$ , may have a different value at each occurrence. Moreover, we use the notation  $\langle F, v \rangle$  to indicate the action of  $F \in V'$  on the element  $v \in V$ ,  $V$  and  $V'$  being different couples of dual reflexive Hilbert spaces, whose precise definition will be clear from the context.

## 2. THE NONCONFORMING VIRTUAL ELEMENT METHOD

We consider the Poisson problem with homogeneous Dirichlet boundary conditions for the scalar unknown  $u$ :

$$-\Delta u = f \text{ in } \Omega, \quad (6a)$$

$$u = 0 \text{ on } \Gamma, \quad (6b)$$

where we assume that  $f \in L^2(\Omega)$ .

Let  $H_0^1(\Omega)$  denote, as usual, the linear subspace of functions of  $H^1(\Omega)$  with zero trace on  $\Gamma$ . The variational formulation of problem (6a)-(6b) reads as:

$$\text{find } u \in H_0^1(\Omega) \text{ such that } a(u, v) = (f, v) \quad \forall v \in H_0^1(\Omega), \quad (7)$$

where the bilinear form  $a(\cdot, \cdot) : H^1(\Omega) \times H^1(\Omega) \rightarrow \mathbb{R}$  is given by

$$a(u, v) = \int_{\Omega} \nabla u \cdot \nabla v, \quad \forall u, v \in H^1(\Omega). \quad (8)$$

The essential Dirichlet boundary condition (6b) is incorporated in the definition of the functional space  $H_0^1(\Omega)$ .

To formulate the nonconforming virtual element approximation of variational problem (7), we need three mathematical objects:

- the virtual element space  $V_k^h$ , which is a finite-dimensional subspace of the nonconforming space  $H_k^{1,nc}(\Omega_h)$ , suitably incorporating a weak form of the homogeneous boundary conditions;
- the virtual element bilinear form  $a_h(\cdot, \cdot) : V_k^h \times V_k^h \rightarrow \mathbb{R}$ , which approximates the bilinear form  $a(\cdot, \cdot)$ . We require  $a_h(\cdot, \cdot)$  to be coercive, continuous, and computable from the degrees of freedom of its arguments;
- an element  $f_h$  of the dual space  $(H_k^{1,nc}(\Omega_h))'$ , which approximates the forcing term  $f$ .

Given these objects, according to the variational form of the continuous problem in (7), the virtual element method reads as:

$$\text{Find } u_h \in V_k^h \text{ such that } a_h(u_h, v) = \langle f_h, v \rangle \quad \forall v \in V_k^h. \quad (9)$$

In the following sections we recall the definition of the nonconforming virtual element space  $V_k^h$ , and of the bilinear form  $a_h$ .

**2.1. The nonconforming virtual element space.** Let  $P$  be a generic element of the mesh  $\Omega_h$  and  $k \geq 1$  an integer number. We define the nonconforming virtual element space on  $P$  (see [7]) as

$$V_k^h(P) = \left\{ v \in H^1(P) : \frac{\partial v}{\partial \mathbf{n}} \in \mathbb{P}_{k-1}(e) \ \forall e \subset \mathcal{E}_P, \Delta v \in \mathbb{P}_{k-2}(P) \right\}, \quad (10)$$

and its “modified” or “enhanced” variant (see [2, 35]) as

$$V_k^{h,\text{en}}(P) = \left\{ v \in H^1(P) : \frac{\partial v}{\partial \mathbf{n}} \in \mathbb{P}_{k-1}(e) \ \forall e \subset \mathcal{E}_P, \Delta v \in \mathbb{P}_k(P), \int_P (v - \Pi_k^{\nabla, P} v) m_\alpha = 0 \quad \forall m_\alpha \in \mathcal{M}_k(P) \setminus \mathcal{M}_{k-2}(P) \right\}. \quad (11)$$

We recall that  $\mathcal{M}_k(P) \setminus \mathcal{M}_{k-2}(P)$ , in the definition above, is the subset of the scaled monomials of degree equal to  $k-1$  and  $k$ .

The following key properties hold for  $V_k^h(P)$  and  $V_k^{h,\text{en}}(P)$ :

- (i) the polynomial space  $\mathbb{P}_k(P)$  is a subspace of both  $V_k^h(P)$  and  $V_k^{h,\text{en}}(P)$ ;
- (ii) the virtual element functions in both  $V_k^h(P)$  and  $V_k^{h,\text{en}}(P)$  are uniquely determined by the following set of *degrees of freedom*:

**(D1)** the values of the polynomial moments of  $v$  of order up to  $k-1$  on each edge  $e \in \mathcal{E}_P$ :

$$\frac{1}{h_e} \int_e v m_\alpha \quad \forall m_\alpha \in \mathcal{M}_{k-1}(e), \forall e \in \mathcal{E}_P; \quad (12)$$

**(D2)** the values of the polynomial moments of  $v$  of order up to  $k-2$  on  $P$ :

$$\frac{1}{|P|} \int_P v m_\alpha \quad \forall m_\alpha \in \mathcal{M}_{k-2}(P). \quad (13)$$

**Remark 2.1.** Other choices are possible for the degrees of freedom. In **(D1)** and **(D2)** the sets  $\mathcal{M}_{k-1}(e)$  and  $\mathcal{M}_{k-2}(P)$  can be replaced with any other basis for the spaces  $\mathbb{P}_{k-1}(e)$  and  $\mathbb{P}_{k-2}(P)$ . We point out that the stabilizing bilinear terms that we are going to construct do not depend on the particular basis chosen and that the bounds that we will prove hold independently of such a choice.

Property (i) is a direct consequence of the space definition and guarantees the optimal order of approximation. Property (ii) has been proven in [7].

The polynomial projection  $\Pi_k^{\nabla, P} v$  is computable using only the values from the linear functionals in **(D1)–(D2)**. We recall that for  $k > 1$ , the average of functions in  $V_k^h(P)$  is computable, and we could replace (5) with the condition that  $\Pi_k^{\nabla, P} v - v$  is average free in  $P$ .

The *global nonconforming virtual element space*  $V_k^h$  of order  $k \geq 1$  subordinate to the mesh  $\Omega_h$  is obtained by gluing together the elemental spaces  $V_k^h(P)$  to form a subspace of the nonconforming space  $H_k^{1,nc}(\Omega_h)$ . The formal definition reads as:

$$V_k^h := \left\{ v \in H_k^{1,nc}(\Omega_h) : v|_P \in V_k^h(P), \forall P \in \Omega_h, \int_e v q = 0, \forall q \in \mathbb{P}_{k-1}(e), \forall e \in \mathcal{E}_\Gamma \right\}. \quad (14)$$

The boundary conditions are enforced in weak form in the definition of the space, by requiring that, for all boundary edges  $e \in \mathcal{E}_\Gamma$ ,  $v|_e$  is orthogonal to the space of polynomials of degree at most  $k-1$  on  $e$ . A similar definition holds for the global space  $V_k^{h,\text{en}}$ , obtained by gluing together the elemental spaces  $V_k^{h,\text{en}}(P)$ . The set of degrees of freedom for  $V_k^h$  and  $V_k^{h,\text{en}}$  is given by collecting the values

**(D1)** for all the mesh edges and **(D2)** for all the mesh elements. The unisolvence of such degrees of freedom in the global space  $V_k^h$  follows from the unisolvence of the degrees of freedom **(D1)–(D2)** in each elemental space, cf. [7].

**2.2. Virtual element discretization.** Hereafter, we only detail the formulation of the virtual element discretization for the *nonenhanced* space  $V_k^h(P)$ . The corresponding formulation for the enhanced space  $V_k^{h,\text{en}}$  is identical.

The virtual element approximation is defined on the broken Sobolev space  $H_k^{1,nc}(\Omega_h)$ . Since the functions of this space can be discontinuous at the elemental boundaries  $\partial P$ , we extend the bilinear form  $a(\cdot, \cdot)$  to the broken Sobolev space  $H^1(\Omega_h)$  as follows:

$$a(u, v) = \sum_{P \in \Omega_h} a^P(u, v) = \sum_{P \in \Omega_h} \int_P \nabla u \cdot \nabla v \quad \forall u, v \in H^1(\Omega_h).$$

The discrete bilinear form  $a_h(\cdot, \cdot)$  is given by the sum of elemental contributions

$$a_h(u, v) = \sum_{P \in \Omega_h} a_h^P(u, v), \quad (15)$$

with

$$a_h^P(u, v) = a^P(\Pi_k^{\nabla, P} u, \Pi_k^{\nabla, P} v) + \sigma^P((I - \Pi_k^{\nabla, P})u, (I - \Pi_k^{\nabla, P})v), \quad (16)$$

where  $\sigma^P(\cdot, \cdot)$  can be any computable, symmetric and positive semidefinite bilinear form such that

$$C_* a^P(v, v) \leq \sigma^P(v, v) \leq C^* a^P(v, v) \quad \forall v \in V_k^h(P) \cap \ker(\Pi_k^{\nabla, P}) \quad (17)$$

for some pair of positive constants  $C_*$  and  $C^*$  that are independent of  $P$  and  $h$ , where  $\ker(\Pi_k^{\nabla, P}) = \{v \in H^1(P) : \Pi_k^{\nabla, P} v = 0\}$  is the kernel of the projection operator  $\Pi_k^{\nabla, P}$ .

Provided (17) holds, the discrete bilinear form  $a_h^P(\cdot, \cdot)$  satisfies the following properties:

- *k*-consistency: for all  $v \in V_k^h(P)$  and for all  $q \in \mathbb{P}_k(P)$  it holds that

$$a_h^P(v, q) = a^P(v, q); \quad (18)$$

- *stability*: there exist two positive constants  $(\alpha_*, \alpha^*)$ , independent of  $P$  and  $h$ , such that

$$\alpha_* a^P(v, v) \leq a_h^P(v, v) \leq \alpha^* a^P(v, v) \quad \forall v \in V_k^h(P). \quad (19)$$

In particular, the first term in the definition of  $a_h^P$  in (16) provides the *k*-consistency of the method, i.e., the exactness on polynomials of degree  $k$ , which follows from the invariance of  $\Pi_k^{\nabla, P}$  on polynomials. The second term in the definition of  $a_h^P$  ensures the stability of the method, cf. also [7], and is zero if one of its two entries is a polynomial of degree at most  $k$ . The stability property follows from a straightforward calculation, by taking  $\alpha^* = \max(1, C^*)$  and  $\alpha_* = \min(1, C_*)$ , cf. [8].

As far as the right-hand side is concerned, we approximate  $f$  with  $f_h$  such that  $\langle f_h, v \rangle$  is computable (we refer to [7, 8] for more details).

In this setting, we can prove the abstract convergence result stated in Theorem 2.2 below. We report this result omitting its proof, which can be found in [7].

**Theorem 2.2** (Abstract convergence result). *Let  $u \in V$  be the solution to problem (7) and  $u_h \in V_k^h$  (or  $V_k^{h,en}$ ) be the solution to problem (7) in the nonconforming setting introduced above. Then, it holds that*

$$\begin{aligned} \alpha_* \|u - u_h\|_{1,h} &\leq \sup_{w \in V_k^h \setminus \{0\}} \frac{|\langle f_h, w_h \rangle - (f, w_h)|}{|w_h|_{1,h}} + \sup_{w \in V_k^h \setminus \{0\}} \frac{|\mathcal{N}(u, w_h)|}{|w_h|_{1,h}} \\ &\quad + \alpha^* \inf_{v \in V_k^h} |u - v|_{1,h} + (\alpha^* + 1) \inf_{q \in \mathbb{P}_{\Omega_h}} |u - q|_{1,h}. \end{aligned} \quad (20)$$

where  $\alpha_*$  and  $\alpha^*$  are defined in (19), and  $\mathcal{N}(u; \cdot)$  is the continuous linear functional

$$\mathcal{N}(u; w_h) = a(u, w_h) - (f, w_h),$$

which defines the conformity error for every virtual element function  $w_h$  in  $V_k^h$  or  $V_k^{h,en}$ .

Bounds on the different terms on the right hand side are provided in [7] and, if the solution  $u$  is smooth, they yield optimal error estimates, provided  $(1 + \alpha^*)/\alpha_*$  is bounded uniformly in  $h$ . The aim of this paper is to design the stabilization term  $\sigma^P$  so that this holds true.

### 3. ALGEBRAIC CONSTRUCTION OF SEMI-INNER PRODUCTS AND SEMI-NORMS IN ABSTRACT FINITE DIMENSIONAL SUBSPACES

The focus of this paper is on the construction of suitable bilinear forms  $\sigma^P$  satisfying (17) under conditions on the mesh  $\Omega_h$  as weak as possible. This problem has been addressed in [13] for the conforming virtual element method. In that case, after showing that it is sufficient for the stabilizing bilinear form to only act on the trace of the virtual function on  $\partial P$ , one can take advantage of the computability of such traces, which are known piecewise polynomials. In the nonconforming case, we have an additional difficulty: contrary to what happens in the conforming case, the trace on  $\partial P$  of the nonconforming virtual element functions is not computable, and we only have access to the degrees of freedom, which correspond to known functionals in the space  $(H^1(P))'$ . Our idea is to design suitable bilinear forms on the space spanned by such functionals and build the stabilization term by a duality technique first introduced in [20], which, in this section, we present in a general abstract setting.

Let  $V$  be a Hilbert space and  $V'$  its dual space, respectively endowed with the inner products  $(\cdot, \cdot)$  and  $(\cdot, \cdot)_*$ , and the induced norms  $\|\cdot\|$  and  $\|\cdot\|_*$ . We denote the duality product by  $\langle \cdot, \cdot \rangle$  and use Roman fonts for the elements of  $V$  and Greek fonts for the elements of  $V'$ . In addition, we consider:

- a continuous seminorm  $|\cdot| : V \rightarrow \mathbb{R}^+$  with kernel  $\widehat{W} \subset V$ ; without loss of generality, after possibly multiplying the seminorm by a fixed constant, we can assume that  $|\cdot| \leq \|\cdot\|$ ;
- a projection operator  $\widehat{\Pi} : V \rightarrow \widehat{W}$ , which is linear, bounded and idempotent, i.e.,

$$\|\widehat{\Pi}v\| \leq C_{\widehat{\Pi}}\|v\| \quad \text{for every } v \in V, \quad \text{and} \quad \widehat{\Pi}^2 = \widehat{\Pi};$$

- the seminorm  $|\cdot|_* : V' \rightarrow \mathbb{R}^+$ , defined by duality with the seminorm  $|\cdot|$ :

$$\forall \eta \in V' : |\eta|_* = \sup_{v \in \ker(\widehat{\Pi})} \frac{\langle \eta, v \rangle}{|v|}; \quad (21)$$

- the projection operator  $\widehat{\Pi}^* : V' \rightarrow V'$ , which is the adjoint of  $\widehat{\Pi}$  with respect to the duality product  $\langle \cdot, \cdot \rangle$ :

$$\langle \widehat{\Pi}^* \eta, v \rangle = \langle \eta, \widehat{\Pi} v \rangle \quad \forall \eta \in V', v \in V.$$

This definition implies that the operator  $\widehat{\Pi}^*$  is also linear, bounded and idempotent, i.e.,

$$\|\widehat{\Pi} \eta\|_* \leq C_{\widehat{\Pi}} \|\eta\|_* \quad \text{for every } \eta \in V', \quad \text{and} \quad (\widehat{\Pi}^*)^2 = \widehat{\Pi}^*.$$

We make the following assumptions:

- (A1) the space  $\widehat{W} = \ker(|\cdot|)$  is finite dimensional;
- (A2) a Poincaré type inequality of the form  $\|v\| \leq C_{\text{poi}}|v|$  holds on  $\ker(\widehat{\Pi})$ .

Assumptions (A1)–(A2) and the previous definitions imply that

- the subspace  $\widehat{W}^* = \widehat{\Pi}^*(V') \subset V'$  is finite dimensional and coincides with the kernel of the dual seminorm  $|\cdot|_*$ , i.e.,  $\widehat{W}^* = \ker(|\cdot|_*)$ ;
- the following equivalence relations in  $V$  holds:

$$|v| = |v - \widehat{\Pi}v| \leq \|v - \widehat{\Pi}v\| \leq C_{\text{poi}}|v| \quad \forall v \in V, \quad (22)$$

from which, by triangular inequality, we can prove the Poincaré-like inequality

$$\|v\| \leq C_{\text{poi}}|v| + \|\widehat{\Pi}v\| \quad \forall v \in V;$$

- the following equivalence relations in  $V'$  holds:

$$C_{\text{poi}}^{-1}|\eta|_* = C_{\text{poi}}^{-1}|\eta - \widehat{\Pi}^*\eta|_* \leq \|\eta - \widehat{\Pi}^*\eta\|_* \leq |\eta|_* \quad \forall \eta \in V'; \quad (23)$$

- the seminorm  $|\cdot|$  and the seminorm defined in  $V$  by duality with the seminorm  $|\cdot|_*$  in  $V'$  are equals:

$$|v| = \sup_{\eta \in \ker(\widehat{\Pi}^*)} \frac{\langle v, \eta \rangle}{|\eta|_*}; \quad (24)$$

- the identity and inequality chain

$$|\langle \eta, v \rangle| = \left| \langle \eta - \widehat{\Pi}^*\eta, v \rangle \right| = \left| \langle \eta, v - \widehat{\Pi}v \rangle \right| \leq |\eta|_* |v - \widehat{\Pi}v| = |\eta|_* |v| \quad (25)$$

holds for every  $\eta \in \ker(\widehat{\Pi}^*)$  and  $v \in V$  and follows from the definition of the seminorms  $|v|$  and  $|\eta|_*$ , and (22)-(23).

We now introduce two finite dimensional subspaces  $W \subset V$  and  $W^* \subset V'$ , and make the further assumptions:

- (A3)  $\widehat{W} \subset W$  and  $\widehat{W}^* \subset W^*$ ;

- (A4) the two following inf-sup conditions hold for the pair of spaces  $W$  and  $W^*$ :

$$\inf_{w \in W} \sup_{\eta \in \widehat{W}^*} \frac{\langle \eta, w \rangle}{\|\eta\|_* \|w\|} \geq \beta \quad \text{and} \quad \inf_{\eta \in \widehat{W}^*} \sup_{w \in W} \frac{\langle \eta, w \rangle}{\|\eta\|_* \|w\|} \geq \beta. \quad (26)$$

Remark that if both inf-sup conditions hold, then we have that  $\dim(W) = \dim(W^*)$ . On the other hand, if  $\dim(W) = \dim(W^*)$ , then either one of the two inf-sup conditions in (26) implies the other.

Furthermore, using the inf-sup conditions above we can prove the equivalence relation in  $W^*$ :

$$C_{\text{poi}}^{-1} \beta |\eta|_* \leq \sup_{w \in W \cap \ker(\widehat{\Pi})} \frac{\langle \eta, w \rangle}{|w|} \leq |\eta|_* \quad \forall \eta \in W^*. \quad (27)$$

Let now  $N = \dim(W) = \dim(W^*)$  and  $M = \dim(\widehat{W}) = \dim(\widehat{W}^*)$ . We consider a set of elements  $\mathfrak{B} = \{e_m\}_{m=1,\dots,N}$ , forming a basis for the space  $W$ , and the corresponding set of elements  $\mathfrak{B}^* = \{\eta_n\}_{n=1,\dots,N}$ , forming a basis for the space  $W^*$  and satisfying the biorthogonality property

$$\langle \eta_n, e_m \rangle = \delta_{n,m} \quad m, n = 1, \dots, N. \quad (28)$$

The validity of the inf-sup condition (26) implies that such a basis  $\mathfrak{B}^*$  exists. Analogously, we will consider a set of elements  $\widehat{\mathfrak{B}} = \{\widehat{e}_j\}_{j=1,\dots,M}$ , forming a basis for  $\widehat{W}$  and the corresponding set of elements  $\widehat{\mathfrak{B}}^* = \{\widehat{\eta}_i\}_{i=1,\dots,M}$ , forming a basis for the space  $\widehat{W}^*$ , and such that, for all  $v \in V$ , we have

$$\widehat{\Pi}v = \sum_{i=1}^M \langle \widehat{\eta}_i, v \rangle \widehat{e}_i. \quad (29)$$

As  $\widehat{\Pi}$  is a projector, the basis sets  $\widehat{\mathfrak{B}}$  and  $\widehat{\mathfrak{B}}^*$  satisfy a biorthogonality property analogous to (28).

As  $\mathfrak{B}$  and  $\mathfrak{B}^*$  are bases for  $W$  and  $W^*$ , we can expand any  $v \in W$  and  $\zeta \in W^*$  as:

$$v = \sum_{m=1}^N v_m e_m \quad \text{and} \quad \zeta = \sum_{n=1}^N \zeta_n \eta_n.$$

The  $N$ -sized vectors  $\mathbf{v} = (v_m)$  and  $\boldsymbol{\zeta} = (\zeta_n)$  collect the expansion coefficients of  $v$  and  $\zeta$  and are respectively referred to as *the vector representations* of  $v$  and  $\zeta$ . We will use an analogous notations for the elements of  $\widehat{W}$  and  $\widehat{W}^*$ , which will be represented by  $M$ -sized vectors collecting the coefficients of their expansions in terms of the bases  $\widehat{\mathfrak{B}}$  and  $\widehat{\mathfrak{B}}^*$ . According with this basis choice, thanks to the biorthogonality property, we can express the duality product between  $\zeta \in W^*$  and  $v \in W$  as follows:

$$\langle \zeta, v \rangle = \boldsymbol{\zeta}^T \mathbf{v}. \quad (30)$$

Now, we consider a symmetric and positive semidefinite matrix  $\mathbf{S} \in \mathbb{R}^{N \times N}$  and the bilinear form  $s(\cdot, \cdot) : W \times W \rightarrow \mathbb{R}$  defined by

$$s(v, w) = \mathbf{w}^T \mathbf{S} \mathbf{v}, \quad (31)$$

where  $\mathbf{v}, \mathbf{w} \in \mathbb{R}^N$  are the vector representations of  $v, w \in W$ . We assume that there exist positive constants  $A$  and  $\alpha$  such that for all  $v, w \in W$

$$s(v, w) \leq A|v| |w| \quad \text{and} \quad \alpha|v|^2 \leq s(v, v). \quad (32)$$

We next introduce a reflexive generalized inverse  $\mathbf{S}^\dagger \in \mathbb{R}^{N \times N}$  of  $\mathbf{S}$ , which we define as follows. Let  $\mathbf{P} \in \mathbb{R}^{M \times N}$  be the matrix representation of the projection operator  $\widehat{\Pi}$ , defined in such a way that  $\mathbf{P}\mathbf{w} \in \mathbb{R}^M$  is the vector representing  $\widehat{\Pi}w \in \widehat{W}$  if  $\mathbf{w} \in \mathbb{R}^N$  is the vector representing  $w \in W$ . The matrix  $\mathbf{P}$  has maximum rank, i.e.  $\text{rank}(\mathbf{P}) = \min(M, N) = M$ , and it projects onto the kernel of  $\mathbf{S}$ , which coincides with the kernel of  $|\cdot|$ .

Then, given  $\boldsymbol{\eta} \in \mathbb{R}^N$ , the saddle point problem

$$\begin{cases} \mathbf{S}\mathbf{w} + \mathbf{P}^T \boldsymbol{\lambda} &= \boldsymbol{\eta}, \\ \mathbf{P}\mathbf{w} &= \mathbf{0}, \end{cases} \quad (33)$$

has a unique solution  $(\mathbf{w}, \boldsymbol{\lambda}) \in \mathbb{R}^N \times \mathbb{R}^M$ , and the corresponding coefficient matrix is nonsingular [28]. Then, we set

$$\mathbf{S}^\dagger \boldsymbol{\eta} = \mathbf{w} \quad \text{with } (\mathbf{w}, \boldsymbol{\lambda}) \in \mathbb{R}^N \times \mathbb{R}^M \text{ solution to (33),} \quad (34)$$

or, equivalently

$$\mathbf{S}^\dagger \boldsymbol{\eta} = (\mathbf{I} \ 0) \begin{pmatrix} \mathbf{S} & \mathbf{P}^T \\ \mathbf{P} & \mathbf{0} \end{pmatrix}^{-1} \begin{pmatrix} \mathbf{I} \\ \mathbf{0} \end{pmatrix} \boldsymbol{\eta}, \quad (35)$$

which gives us

$$\mathbf{S}^\dagger = (\mathbf{I} \ 0) \begin{pmatrix} \mathbf{S} & \mathbf{P}^T \\ \mathbf{P} & \mathbf{0} \end{pmatrix}^{-1} \begin{pmatrix} \mathbf{I} \\ \mathbf{0} \end{pmatrix},$$

from which we also deduce that  $\mathbf{S}^\dagger$  is a symmetric matrix.

In this setting, the saddle point problem (33) is well posed, and  $\mathbf{w} = \mathbf{S}^\dagger \boldsymbol{\eta} \in \mathbb{R}^N$  if and only if there exists a vector  $\boldsymbol{\lambda} \in \mathbb{R}^M$  such that the pair  $(\mathbf{w}, \boldsymbol{\lambda})$  satisfies (33). By exploiting such a fact, it can be shown that the matrices  $\mathbf{S}$  and  $\mathbf{S}^\dagger$  satisfy the identities

$$\mathbf{S}\mathbf{S}^\dagger \mathbf{S} = \mathbf{S} \quad \text{and} \quad \mathbf{S}^\dagger \mathbf{S}\mathbf{S}^\dagger = \mathbf{S}^\dagger, \quad (36)$$

so that  $\mathbf{S}^\dagger$  is indeed a reflexive generalized inverse of  $\mathbf{S}$  and viceversa. If  $\mathbf{P}^* \in \mathbb{R}^{M \times N}$  is the matrix representing  $\widehat{\Pi}^*$ , we can prove that

$$\mathbf{S}^\dagger \mathbf{S} = \mathbf{I}_N - (\mathbf{P}^*)^T \mathbf{P}, \quad (37)$$

where  $\mathbf{I}_N \in \mathbb{R}^{N \times N}$  is the identity matrix.

Using the biorthogonality property (28), we can show that  $\mathbf{P}^*$  coincides with the matrix representing the inclusion of  $\widehat{W}$  into  $W$ : if  $\widehat{\mathbf{w}} \in \widehat{W} \subset W$  is written as

$$\widehat{\mathbf{w}} = \sum_{i=1}^M \widehat{w}_i \widehat{e}_i = \sum_{n=1}^N w_n e_n,$$

the vectors  $\widehat{\mathbf{w}} = (\widehat{w}_i)$  and  $\mathbf{w} = (w_n)$  satisfy  $\mathbf{w} = \mathbf{P}^* \widehat{\mathbf{w}}$ . We can then see that the matrix  $\mathbf{I}_N - (\mathbf{P}^*)^T \mathbf{P}$  represents the operator  $(\mathbf{I} - \widehat{\Pi})$ .

**Remark 3.1.** The projector  $\widehat{\Pi}$  has different matrix representations, depending on whether it is seen as an operator from  $W$  to  $\widehat{W}$  or as an operator from  $W$  to  $W$ . In the first case,  $\widehat{\Pi} \mathbf{w}$  is represented with respect to the basis  $\widehat{\mathcal{B}}$  and the operator is represented by the  $M \times N$  matrix  $\mathbf{P}$ . In the second case, the basis used to express  $\widehat{\Pi} \mathbf{w}$  is  $\mathcal{B}$  and the operator is represented by the  $N \times N$  matrix  $(\mathbf{P}^*)^T \mathbf{P}$ . An analogous observation holds for the operator  $\widehat{\Pi}^*$ .

We have now all the ingredients to define a bilinear form on  $W^*$  acting, on such a subspace, as a semi-inner product inducing a semi-norm equivalent to the dual semi-norm  $|\cdot|_*$ . More precisely, the bilinear form  $s^* : W^* \times W^* \rightarrow \mathbb{R}$  is defined by

$$s^*(\boldsymbol{\eta}, \boldsymbol{\zeta}) = \boldsymbol{\eta}^T \mathbf{S}^\dagger \boldsymbol{\zeta},$$

where, once again,  $\boldsymbol{\eta}, \boldsymbol{\zeta} \in \mathbb{R}^N$  are the vector representation of  $\boldsymbol{\eta}, \boldsymbol{\zeta} \in W^*$ . As  $\mathbf{S}^\dagger$  is symmetric and positive semidefinite,  $s^*(\cdot, \cdot)$  is indeed a semi-inner product on  $W^*$ , and we have the following Proposition.

**Proposition 3.2.** *For every  $\eta, \zeta \in W^*$ , it holds that*

$$C_{\text{poi}}^{-2} A^{-1} \beta^2 |\eta|_* \leq s^*(\eta, \eta), \quad \text{and} \quad s^*(\eta, \zeta) \leq \alpha^{-1} |\eta|_* |\zeta|_*. \quad (38)$$

*Proof.* Let  $\eta \in W^*$  and  $w \in W \cap \ker(\widehat{\Pi})$  with vector representations  $\boldsymbol{\eta}, \mathbf{w} \in \mathbb{R}^N$ , and recall that  $(\mathbf{I}_N - (\mathbf{P}^*)^T \mathbf{P}) \mathbf{w}$  is the vector representation of  $w - \widehat{\Pi}w$ . Since  $\widehat{\Pi}w = 0$ , (37) yields

$$\langle \eta, w \rangle = \langle \eta, w - \widehat{\Pi}w \rangle = \boldsymbol{\eta}^T (\mathbf{I}_N - (\mathbf{P}^*)^T \mathbf{P}) \mathbf{w} = \boldsymbol{\eta}^T \mathbf{S}^\dagger \mathbf{S} \mathbf{w}.$$

The matrix  $\mathbf{S}^\dagger$  is symmetric and positive semidefinite, so there exists a  $N \times N$  matrix  $\mathbf{G}$  such that  $\mathbf{S}^\dagger = \mathbf{G}^T \mathbf{G}$ . We substitute such decomposition, we apply the Cauchy-Schwarz inequality and the first identity of (36), and we find that

$$\begin{aligned} \boldsymbol{\eta}^T \mathbf{S}^\dagger \mathbf{S} \mathbf{w} &= (\mathbf{G} \boldsymbol{\eta})^T (\mathbf{G} \mathbf{S} \mathbf{w}) \leq \sqrt{\boldsymbol{\eta}^T \mathbf{G}^T \mathbf{G} \boldsymbol{\eta}} \sqrt{\mathbf{w}^T \mathbf{S}^T \mathbf{G}^T \mathbf{G} \mathbf{S} \mathbf{w}} = \sqrt{\boldsymbol{\eta}^T \mathbf{S}^\dagger \boldsymbol{\eta}} \sqrt{\mathbf{w}^T \mathbf{S}^\dagger \mathbf{S} \mathbf{w}} \\ &= \sqrt{\boldsymbol{\eta}^T \mathbf{S}^\dagger \boldsymbol{\eta}} \sqrt{\mathbf{w}^T \mathbf{S} \mathbf{w}} \leq A^{1/2} \sqrt{\boldsymbol{\eta}^T \mathbf{S}^\dagger \boldsymbol{\eta}} |w|. \end{aligned}$$

Then for  $w \in W \cap \ker(\widehat{\Pi})$  we have that

$$\frac{\langle \eta, w \rangle}{|w|} \leq A^{1/2} \sqrt{\boldsymbol{\eta}^T \mathbf{S}^\dagger \boldsymbol{\eta}},$$

and, using the lower bound in (27), we find that for every  $\eta \in W^*$

$$|\eta|_* \leq C_{\text{poi}} \beta^{-1} \sup_{w \in W \cap \ker(\widehat{\Pi})} \frac{\langle \eta, w \rangle}{|w|} \leq C_{\text{poi}} \beta^{-1} A^{1/2} \sqrt{\boldsymbol{\eta}^T \mathbf{S}^\dagger \boldsymbol{\eta}},$$

which gives us the first bound in (38). Conversely, for any given  $\eta \in W^*$  and its vector representation  $\boldsymbol{\eta} \in \mathbb{R}^N$ , we let  $w \in W$  be the element with vector representation  $\mathbf{w} = \mathbf{S}^\dagger \boldsymbol{\eta}$ . Then, we start from the vector representation of the duality product (30), use inequality (25), the matrix representation of  $w$  in (31), and the second identity of (36) and, since, by the definition of  $\mathbf{S}^\dagger$ ,  $w \in \ker(\widehat{\Pi})$ , we can write:

$$\begin{aligned} \boldsymbol{\eta}^T \mathbf{S}^\dagger \boldsymbol{\eta} &= \boldsymbol{\eta}^T \mathbf{w} = \langle \eta, w \rangle \leq |\eta|_* |w| \leq \alpha^{-1/2} |\eta|_* \sqrt{\mathbf{w}^T \mathbf{S} \mathbf{w}} \\ &= \alpha^{-1/2} |\eta|_* \sqrt{\boldsymbol{\eta}^T \mathbf{S}^\dagger \mathbf{S} \mathbf{w}} = \alpha^{-1/2} |\eta|_* \sqrt{\boldsymbol{\eta}^T \mathbf{S}^\dagger \boldsymbol{\eta}}. \end{aligned}$$

We divide both sides by  $\sqrt{\boldsymbol{\eta}^T \mathbf{S}^\dagger \boldsymbol{\eta}}$  and obtain that  $\sqrt{\boldsymbol{\eta}^T \mathbf{S}^\dagger \boldsymbol{\eta}} \leq \alpha^{-1/2} |\eta|_*$ . Analogously, we have that  $\sqrt{\boldsymbol{\zeta}^T \mathbf{S}^\dagger \boldsymbol{\zeta}} \leq \alpha^{-1/2} |\zeta|_*$ .

Then, to prove the second relation in (38), we simply apply the Cauchy-Schwartz inequality and the above bounds, and we obtain

$$s^*(\eta, \zeta) = \boldsymbol{\zeta}^T \mathbf{S}^\dagger \boldsymbol{\eta} \leq \sqrt{\boldsymbol{\zeta}^T \mathbf{S}^\dagger \boldsymbol{\zeta}} \sqrt{\boldsymbol{\eta}^T \mathbf{S}^\dagger \boldsymbol{\eta}} \leq \alpha^{-1} |\eta|_* |\zeta|_*.$$

□

**Remark 3.3.** We can also use the above approach to build a semi-inner product equivalent to  $|\cdot|$  in any finite dimensional subspace  $\widetilde{W} \subset V$  containing  $\widehat{W}$  and verifying inf-sup conditions of the form (26), with  $\widetilde{W}$  replacing  $W$ . By applying the same reasoning as above with the roles of  $V$  and  $V'$  switched, we introduce the reflexive generalized inverse  $\mathbf{S}^{\dagger\dagger}$  of  $\mathbf{S}^\dagger$  defined as

$$\mathbf{S}^{\dagger\dagger} = (\mathbf{I} \ 0) \begin{pmatrix} \mathbf{S}^\dagger & (\mathbf{P}^*)^T \\ \mathbf{P}^* & \mathbf{0} \end{pmatrix}^{-1} \begin{pmatrix} \mathbf{I} \\ \mathbf{0} \end{pmatrix},$$

where  $P^*$  is the matrix realizing the adjoint projector  $\widehat{\Pi}^*$ . Under our assumptions it is possible to prove that  $S^{\dagger\dagger} = S$ . Then, we define the bilinear form  $\tilde{s} : \widetilde{W} \times \widetilde{W} \rightarrow \mathbb{R}$  as

$$\tilde{s}(\tilde{w}, \tilde{v}) := \mathbf{v}^T S^{\dagger\dagger} \mathbf{w} = \mathbf{v}^T S \mathbf{w},$$

where  $\mathbf{v}$  and  $\mathbf{w}$  are, this time, the vectors representing the functions  $\tilde{w}$  and  $\tilde{v}$  with respect to the basis  $\tilde{\mathcal{B}} = \{\tilde{e}_m\}_{m=1,\dots,N}$  for  $\widetilde{W}$ , that is biorthogonal to  $\mathcal{B}^*$ . By applying Proposition 3.2, we find that

$$\tilde{s}(\tilde{v}, \tilde{v}) \gtrsim |v|^2, \quad \tilde{s}(\tilde{v}, \tilde{w}) \lesssim |v| |w|$$

for all  $\tilde{v}, \tilde{w} \in \widetilde{W}$ . The implicit constants in these bounds depend only on the constants  $C_{\text{poi}}$ ,  $A$ ,  $\beta$  and  $\alpha$ , and on the inf-sup constant  $\tilde{\beta}$  relative to the duality between  $W^*$  and  $\widetilde{W}$ . In other words, the “stiffness” matrix  $S$  constructed on  $W$  can be used to define an equivalent semi-inner product on any other subspace  $\widetilde{W} \subset V$  containing  $\widehat{W}$  and verifying an inf-sup conditions of the form (26).

#### 4. STABILIZATION IN THE NONCONFORMING VIRTUAL ELEMENT METHOD

We now focus on the problem of building stabilization terms for the nonconforming virtual element method described in Section 2. The aim is to achieve robustness with respect to the mesh size, under as weak assumptions as possible, on the shape of the elements. We start by making the following minimal shape regularity assumption, which we assume to be always satisfied:

**(G1)** there exist a positive constant  $\gamma_0$  such that for all  $\Omega_h$ , every element  $P \in \Omega_h$  is star-shaped with respect to a ball of radius greater than  $\gamma_0 h_P$ .

We have the following lemma, whose proof is postponed to Appendix A.

**Lemma 4.1.** *Let  $v \in V_k^h(P)$  and  $\hat{v} \in V_k^{h,en}(P)$  be virtual element functions satisfying*

$$\int_e v\eta = \int_e \hat{v}\eta \quad \forall \eta \in \mathbb{P}_{k-1}(e), \forall e \in \mathcal{E}_P, \quad \int_P vq = \int_P \hat{v}q, \quad \forall q \in \mathbb{P}_{k-2}(P). \quad (39)$$

*Then, it holds that*

$$|\hat{v}|_{1,P} \simeq |v|_{1,P}.$$

Thanks to this lemma, we can limit our analysis to the “plain” discretization defined by (10). The construction and the analysis of the new stabilization terms will consist in several steps:

*Step 1.* We show that the nonconforming virtual element space  $V_k^h(P)$  and the subspace  $V_k^*$  of  $(H^1(P))'$  spanned by the functionals yielding the degrees of freedom **(D1)**–**(D2)** are in a stable duality relation, i.e., they satisfy an inf-sup condition of the form (26).

*Step 2.* We next show that, if we restrict ourselves to a suitably chosen subspace  $\mathring{V}_k^h(P)$  of  $V_k^h(P)$ , a similar stable duality relation holds with the subspace spanned by the functionals corresponding to the sole boundary degrees of freedom **(D1)**, which is isomorphic to the subspace  $N_{k-1}(\partial P) \subset H^{-\frac{1}{2}}(\partial P)$  of piecewise polynomials on the boundary mesh  $\mathcal{E}_P$ .

*Step 3.* As  $\ker \Pi_k^{\nabla, P} \subseteq \mathring{V}_k^h(P)$ , putting ourselves in the framework of Section 3, we can then transfer the problem of building the bilinear form  $\sigma^P$  defined on the space  $V_k^h(P)$ , to whose elements we do not have direct access, to the problem of building a  $H^{-\frac{1}{2}}(\partial P)$  semi-inner product on the space  $N_{k-1}(\partial P)$ .

*Step 4.* We finally show that, on  $N_{k-1}(\partial P)$ , the  $H^{-\frac{1}{2}}(\partial P)$  semi inner product can be split as the sum of a global contribution acting on piecewise constants, and local contributions acting on average-free polynomials of degree  $k-1$  on each edge. We postpone the treatment of the former to the next section and, for the latter, we prove that a suitably scaled  $L^2$  inner product yields optimal estimates.

*Mesh assumptions.* Before going into the details of the construction of the stabilization term, we present the precise assumptions on the polygonal tessellations  $\Omega_h$ . As already stated, we assume that **(G1)** is always satisfied. First, we observe that we can write the stabilization proposed in [7] as

$$\sigma^P(u, v) = \mathbf{v}^T \mathbf{u},$$

where  $\mathbf{u}$  and  $\mathbf{v}$  are the vectors collecting the degrees of freedom **(D1)–(D2)** of the virtual element functions  $u$  and  $v$ . This bilinear form satisfies (17), provided that the family of polygonal meshes  $\Omega_h$  satisfies the following additional shape regularity assumption:

**(G2)** there exist a positive constant  $\gamma_1$  such that for all  $\Omega_h$ , the distance between any two vertices of every element  $P \in \Omega_h$  is greater than  $\gamma_1 h_P$ .

Assumption **(G2)** implies that the size of adjacent edges are comparable. It also implies that the number of edges in the boundary of a polygonal element is uniformly bounded from above and the minimum edge length cannot decrease faster than the mesh size  $h$  during the refinement process for  $h \rightarrow 0$ . So, mesh families where the number of edges can become arbitrarily high as  $h \rightarrow 0$  are not admissible. Such an assumption is quite strong, and, to allow more freedom in the choice of the mesh, weaker alternatives have been considered in the literature. Assumption **(G2)** can be replaced by either one of assumptions **(G2a)** and **(G2b)** below. The former assumption allows elements to have a very large number of very small edges; the latter one to have very small edges adjacent to large edges.

**(G2a)** There exists a real positive constant  $\gamma_2$  such that for all meshes  $\Omega_h$  and every pair of adjacent edges  $e, e' \in \mathcal{E}_P, P \in \Omega_h$ , it holds that

$$\frac{1}{\gamma_2} \leq \frac{h_e}{h_{e'}} \leq \gamma_2.$$

**(G2b)** There exists an integer positive constant  $N^*$  such that for all meshes  $\Omega_h$ , every  $P \in \Omega_h$  has at most  $N^*$  edges.

To allow the meshes a greater flexibility, we combine **(G1)** with the following assumption, which essentially requires that, for  $P \in \Omega_h$ , a part of  $\partial P$  satisfies **(G2a)** and the remaining part satisfies **(G2b)**.

**(G3)** There exist two constants  $\gamma_2 > 0$  and  $N^* \in \mathbb{N}$  such that for all  $\Omega_h$ , the edge set  $\mathcal{E}_P$  of every polygon  $P \in \Omega_h$  can be split as  $\mathcal{E}_P = \mathcal{E}_P^1 \cup \mathcal{E}_P^2$ , where  $\mathcal{E}_P^1$  and  $\mathcal{E}_P^2$  are such that

**(G3.1)** the inequality

$$\frac{1}{\gamma_2} \leq \frac{h_e}{h_{e'}} \leq \gamma_2$$

holds for any pair of adjacent edges  $e, e' \in \mathcal{E}_P$  with  $e \in \mathcal{E}_P^1$ ;

**(G3.2)**  $\mathcal{E}_P^2$  contains at most  $N^*$  edges.

Assumption **(G3)** allows for situations where a large number of small edges coexists with some large edges. We can think of families of meshes for which such an assumption is not satisfied, but they would be extremely pathological.

*Step 1. Degrees of freedom: definition and stable duality.* Let  $P \in \Omega_h$ . We devote this section to verifying that the local nonconforming virtual element space  $V_k^h(P) \subset H^1(P)$ , defined by (10), and the space  $V_k^*(P)$  spanned in  $(H^1(P))'$  by the functionals yielding the degrees of freedom **(D1)**–**(D2)** fall into the framework considered in Section 3. To this aim we introduce the space of discontinuous piecewise polynomials of degree  $k-1$  that are defined on the elemental boundary  $\partial P$ ,

$$N_{k-1}(\partial P) = \left\{ \lambda \in L^2(\partial P) : \lambda|_e \in \mathbb{P}_{k-1}(e), \forall e \in \mathcal{E}_P \right\} \subset H^{-\frac{1}{2}}(\partial P),$$

and we let  $V_k^*(P) \subset (H^1(P))'$  be defined as

$$V_k^*(P) = \gamma_P^* N_{k-1}(\partial P) \oplus \mathbb{P}_{k-2}(P) \subset (H^1(P))',$$

where  $\gamma_P^* : H^{-\frac{1}{2}}(\partial P) \rightarrow (H^1(P))'$  is the adjoint of the trace operator  $\gamma_P : H^1(P) \rightarrow H^{\frac{1}{2}}(\partial P)$ : for all  $\xi \in H^{-\frac{1}{2}}(\partial P)$

$$\langle \gamma_P^* \xi, v \rangle = \langle \xi, \gamma_P v \rangle, \quad \forall v \in H^1(P). \quad (40)$$

In fact, for any given virtual elemental function  $v \in V_k^h(P)$ , the degrees of freedom **(D1)**–**(D2)** of  $v$  stem from the action of a basis of  $V_k^*(P)$ .

Let  $H_\emptyset^1(P)$  denote the subspace of functions in  $H^1(P)$  whose integral on the polygonal boundary  $\partial P$  is zero:

$$H_\emptyset^1(P) = \left\{ v \in H^1(P) : \int_{\partial P} v = 0 \right\}$$

where, for the sake of notational simplicity and with some abuse of notation, we let the same symbol  $v$  denote both a function  $v \in H^1(P)$  and its trace on  $\partial P$ . By duality with such a subspace of  $H^1(P)$ , we define the dual seminorm  $|\cdot|_{-1,P} : (H^1(P))' \rightarrow \mathbb{R}^+$  as

$$\forall \eta \in (H^1(P))' : \quad |\eta|_{-1,P} = \sup_{v \in H_\emptyset^1(P)} \frac{\langle \eta, v \rangle}{|v|_{1,P}}.$$

We can prove the following proposition, which is a stronger version of the unisolvency property for the degrees of freedom. In fact, not only it implies unisolvency, but also that the space spanned by the functionals yielding the degrees of freedom provides control, uniformly in  $h$ , on the  $H^1$  norm of the virtual element functions. Let

$$\int_{\partial P} v = \frac{1}{|\partial P|} \int_{\partial P} v$$

denote the average of  $v$  on  $\partial P$ .

**Lemma 4.2.** *For all  $v \in V_k^h(P)$  it holds that*

$$\sup_{\eta \in V_k^*(P)} \frac{\langle \eta, v \rangle}{\sqrt{|\langle \eta, 1 \rangle|^2 + |\eta|_{-1,P}^2}} \geq \sqrt{\left| \int_{\partial P} v \right|^2 + |v|_{1,P}^2}.$$

*Proof.* Let  $v \in V_k^h(P)$  and take  $\eta_v \in V_k^*(P)$  given by

$$\eta_v = \gamma_P^* \nabla v \cdot \mathbf{n}_P - \Delta v + \frac{1}{|\partial P|} \gamma_P^* \int_{\partial P} v.$$

According to (40) and to the definition of  $\eta_v$  given above, for every function  $w \in H^1(P)$  we find that

$$\begin{aligned} \langle \eta_v, w \rangle &= \int_{\partial P} w \nabla v \cdot \mathbf{n}_P - \int_P w \Delta v + \left( \frac{1}{|\partial P|} \int_{\partial P} w \right) \left( \int_{\partial P} v \right) \\ &= \int_{\partial P} \nabla v \cdot \nabla w + \left( \int_{\partial P} w \right) \left( \int_{\partial P} v \right), \end{aligned} \quad (41)$$

which, for  $w \in H_\emptyset^1(P)$ , reduces to

$$\langle \eta_v, w \rangle = \int_{\partial P} \nabla v \cdot \nabla w.$$

Then

$$|\eta_v|_{-1,P} = \sup_{w \in H_\emptyset^1(P)} \frac{\langle \eta_v, w \rangle}{|w|_{1,P}} = \sup_{w \in H_\emptyset^1(P)} \frac{\int_P \nabla v \cdot \nabla w}{|w|_{1,P}} = |v|_{1,P}. \quad (42)$$

Moreover, taking  $w = 1$  in (41) yields

$$\langle \eta_v, 1 \rangle = \int_{\partial P} v. \quad (43)$$

Adding the square of (42) and (43) yields

$$|\langle \eta_v, 1 \rangle|^2 + |\eta_v|_{-1,P}^2 = \left| \int_{\partial P} v \right|^2 + |v|_{1,P}^2, \quad (44)$$

and taking  $w = v$  in (41) gives us the identity

$$\langle \eta_v, v \rangle = \int_P |\nabla v|^2 + \left| \int_{\partial P} v \right|^2.$$

Finally, we combine this identity with (44) to obtain

$$\sqrt{\left| \int_{\partial P} v \right|^2 + |v|_{1,P}^2} = \frac{\langle \eta_v, v \rangle}{\sqrt{|\langle \eta_v, 1 \rangle|^2 + |\eta_v|_{-1,P}^2}} \leq \sup_{\eta \in V_k^*(P)} \frac{\langle \eta, v \rangle}{\sqrt{|\langle \eta, 1 \rangle|^2 + |\eta|_{-1,P}^2}},$$

which holds for every  $v \in V_k^h(P)$  and is the assertion of the lemma.  $\square$

*Step 2. Reduction to the boundary.* If we restrict ourselves to a suitable subspace  $\mathring{V}_k^h(P)$  of  $V_k^h(P)$ , we have a stable duality result with the space spanned by the functionals yielding the boundary degrees of freedom **(D1)**. More precisely, consider the space of harmonic polynomials of degree at most  $k$ ,

$$\mathcal{A}_k(P) = \left\{ q \in \mathbb{P}_k(P) : \Delta q = 0 \right\} \subset \mathbb{P}_k(P),$$

and the space of polynomials of degree at most  $k$  orthogonal to all polynomials in  $\mathcal{A}_k(P)$ ,

$$\mathring{\mathbb{P}}_k(P) = \left\{ p \in \mathbb{P}_k(P) : \int_P pq = 0 \ \forall q \in \mathcal{A}_k(P) \right\} \subset \mathbb{P}_k(P).$$

Let

$$\mathring{V}_k^h(P) = \left\{ v \in V_k^h(P) : \int_P \nabla v \cdot \nabla q = 0, \forall q \in \mathring{\mathbb{P}}_k(P) \right\}. \quad (45)$$

Remark that  $V_k^h(P) \cap \ker \Pi_k^{\nabla, P} \subset \mathring{V}_k^h(P)$ . We have the following lemma.

**Lemma 4.3.** *For all  $v \in \mathring{V}_k^h(P)$  we have*

$$\sup_{\eta \in N_{k-1}(\partial P)} \frac{\langle \gamma_P^* \eta, v \rangle}{\sqrt{|\langle \gamma_P^* \eta, 1 \rangle|^2 + |\gamma_P^* \eta|_{-1,P}^2}} \gtrsim \sqrt{\left| \int_{\partial P} v \right|^2 + |v|_{1,P}^2}.$$

To prove Lemma 4.3, we need two technical lemmas, which have been proven in [13] for the conforming virtual element method and are also true in the nonconforming case. As the proof is the same, we omit it.

**Lemma 4.4.** *The following inverse inequality holds for all  $v \in V_k^h(P)$ :*

$$\|\Delta v\|_{0,P} \lesssim h_P^{-1} |v|_{1,P}.$$

**Lemma 4.5.** *For all  $v \in V_k^h(P)$  there exists a polynomial function  $\tilde{q} \in \mathring{\mathbb{P}}_k(P)$  such that*

$$\Delta \tilde{q} = \Delta v \quad \text{and} \quad |\tilde{q}|_{1,P} \lesssim h_P \|\Delta v\|_{0,P}.$$

We can now prove Lemma 4.3.

*Proof of Lemma 4.3.* Consider a function  $v \in \mathring{V}_k^h(P)$ . Thanks to Lemmas 4.5 and 4.4, there exists a polynomial  $\tilde{q} \in \mathring{\mathbb{P}}_k(P)$  such that

$$\Delta \tilde{q} = \Delta v \quad \text{and} \quad |\tilde{q}|_{1,P} \lesssim h_P \|\Delta v\|_{0,P} \lesssim |v|_{1,P}. \quad (46)$$

We take  $\eta_v \in N_{k-1}(\partial P)$  given by

$$\eta_v = \nabla(v - \tilde{q}) \cdot \mathbf{n}_P + \frac{1}{|\partial P|} \int_{\partial P} v. \quad (47)$$

For any  $w \in H^1(P)$  we have

$$\begin{aligned} \langle \gamma_P^* \eta_v, w \rangle &= \int_{\partial P} \nabla(v - \tilde{q}) \cdot \mathbf{n}_P w + \int_{\partial P} w \frac{1}{|\partial P|} \int_{\partial P} v = \\ &= \int_P \nabla(v - \tilde{q}) \cdot \nabla w + \int_P \Delta(v - \tilde{q}) w + \left( \int v \right) \left( \int w \right) \\ &= \int_P \nabla(v - \tilde{q}) \cdot \nabla w + \left( \int v \right) \left( \int w \right). \end{aligned} \quad (48)$$

As  $v \in \mathring{V}_k^h(P)$ , we then have

$$\langle \gamma_P^* \eta_v, v \rangle = \int_P \nabla(v - \tilde{q}) \cdot \nabla v + \left( \int v \right)^2 = |v|_{1,P}^2 + \left( \int v \right)^2.$$

Moreover, using the triangular inequality and the bound on  $\tilde{q}$  in (46) we see that

$$|\gamma_P^* \eta_v|_{-1,P} = \sup_{w \in H_{\emptyset}^1(P)} \frac{\langle \gamma_P^* \eta_v, w \rangle}{|w|_{1,P}} = \sup_{w \in H_{\emptyset}^1(P)} \frac{\int_P \nabla w \cdot \nabla(v - \tilde{q})}{|w|_{1,P}} = |v - \tilde{q}|_{1,P} \lesssim |v|_{1,P}, \quad (49)$$

and, setting  $w = 1$  in (48),

$$\langle \gamma_P^* \eta_v, 1 \rangle = \int v,$$

which yields

$$|\langle \gamma_P^* \eta_v, 1 \rangle|^2 + |\eta_v|_{-1,P}^2 \lesssim |v|_{1,P}^2 + \left( \int v \right)^2.$$

Then, for every  $v \in \overset{\circ}{V}_k^h(P)$

$$\begin{aligned} \sqrt{|v|_{1,P}^2 + \left( \int v \right)^2} &= \frac{\langle \gamma_P^* \eta_v, v \rangle}{\sqrt{|v|_{1,P}^2 + (\int v)^2}} \lesssim \frac{\langle \gamma_P^* \eta_v, v \rangle}{\sqrt{|\langle \gamma_P^* \eta_v, 1 \rangle|^2 + |\eta_v|_{-1,P}^2}} \\ &\leq \sup_{\eta \in N_{k-1}(\partial P)} \frac{\langle \gamma_P^* \eta, v \rangle}{\sqrt{|\langle \gamma_P^* \eta, 1 \rangle|^2 + |\eta|_{-1,P}^2}} \end{aligned}$$

which is the assertion of the lemma.  $\square$

As the kernel of  $\Pi_k^{\nabla, P}$  is included in  $\overset{\circ}{V}_k^h(P)$ , this will allow us to neglect the interior degrees of freedom **(D2)** when designing the stabilization bilinear form.

We conclude by remarking that we have  $\dim(\overset{\circ}{V}_k^h(P)) = \dim(N_{k-1}(\partial P))$ . Indeed, we have the splitting (cf. [25])

$$\mathbb{P}_k(P) = \mathcal{A}_k(P) \oplus |\mathbf{x}|^2 \mathbb{P}_{k-2}(P),$$

so that  $\dim(\overset{\circ}{\mathbb{P}}_k(P)) = \dim(\mathbb{P}_{k-2}(P))$ , which implies that  $\dim(\overset{\circ}{V}_k^h(P)) \geq \dim(V_k^h(P)) - \dim(\mathbb{P}_{k-2}(P)) = \dim(N_{k-1}(\partial P))$ . The converse inequality is a consequence of Lemma 4.3.

*Step 3. Transfer to the dual.* We use the approach of Section 3 with these definitions:

- $V = (H^1(P))'$  and  $V' = H^1(P)$ ;
- $W = \gamma_P^*(N_{k-1}(\partial P))$  and  $W^* = \overset{\circ}{V}_k^h(P)$ ;
- $\widehat{W} = \gamma_P^*(\mathbb{P}_0(\partial P))$  and  $\widehat{W}^* = \mathbb{P}_0(P)$ .

Remark that  $(H^1(P))'$ , which is naturally a dual space, plays here the role of the primal space, and, vice-versa,  $H^1(P)$  plays the role of the dual space.

The projector operators  $\widehat{\Pi} : (H^1(P))' \rightarrow \gamma_P^*(\mathbb{P}_0(\partial P))$  and  $\widehat{\Pi}^* : H^1(P) \rightarrow \mathbb{P}_0(P)$  are, respectively, defined as

$$\widehat{\Pi}(\eta) = |\partial P|^{-1} \langle \eta, 1 \rangle \gamma_P^*(1) \quad \text{and} \quad \widehat{\Pi}^*(u) = \int_{\partial P} u,$$

(we recall that  $\mathbb{P}_0(\omega)$  is the restriction to  $\omega$  of the space of constant functions).

Thanks to Lemma 4.5, assumptions **(A1)**–**(A4)** are satisfied, provided we endow the spaces  $H^1(P)$  and  $(H^1(P))'$  with the couple of dual norms (cf. [23])

$$\|w\|_{1,P} = \sqrt{\left| \int_{\partial P} v \right|^2 + |v|_{1,P}^2}, \quad \|\zeta\|_{-1,P} = \sqrt{|\langle \zeta, 1 \rangle|^2 + |\zeta|_{-1,P}^2}.$$

In order to build a bilinear form  $\sigma^P$  satisfying (17) on the space  $W^* = \mathring{V}_k^h(P)$ , to whose elements we do not have access (not even to the boundary values), we can instead build a bilinear form  $\sigma_P^*$  on the space  $N_{k-1}(\partial P)$  (whose elements are known in closed form), satisfying

$$\sigma_P^*(\eta, \eta) \simeq |\gamma_P^* \eta|_{-1,P}^2 \quad \text{and} \quad \sigma_P^*(\eta, \mu) \lesssim |\gamma_P^* \eta|_{-1,P} |\gamma_P^* \mu|_{-1,P}. \quad (50)$$

Once  $\sigma_P^*$  is built, we consider:

- the set  $\mathfrak{B} = \{\zeta_i, i = 1, \dots, kN\}$  of the piecewise polynomials of degrees up to  $k-1$  used to evaluate the degrees of freedom **(D1)** associated with the elemental boundary  $\partial P$ . The set  $\mathfrak{B}$  is a basis of the space  $N_{k-1}(\partial P)$ ;
- the basis functions  $\phi_i \in \mathring{V}_k^h(P)$  associated with the elements  $\zeta_i$  of the basis  $\mathfrak{B}$ , verifying

$$\int_{\partial P} \phi_i \zeta_j = \delta_{ij}, \quad i, j = 1, \dots, kN.$$

The value of a degree of freedom of a function in  $\mathring{V}_k^h(P)$  corresponding to the unknown basis function  $\phi_i$  coincides with its  $i$ -th boundary degree of freedom in the complete local VEM space. Then, we apply the framework of Section 3. We let  $\mathbf{S} = (s_{ij})$  denote the stiffness matrix associated to the bilinear form  $s = \sigma_P^*$ , which is

$$s_{ij} = s(\zeta_i, \zeta_j) = \sigma_P^*(\zeta_j, \zeta_i) \quad i, j = 1, \dots, kN,$$

We define matrix  $\Sigma = (s_{ij})$  by  $\Sigma = \mathbf{S}^\dagger$ , where  $\mathbf{S}^\dagger$  is the reflexive generalized inverse of  $\mathbf{S}$  of Section 3, and the bilinear form  $\sigma^P(\cdot, \cdot)$  by setting

$$\sigma^P(\phi_j, \phi_i) = s_{ij} \quad i, j = 1, \dots, kN. \quad (51)$$

Proposition 3.2 states that  $\sigma^P(\cdot, \cdot)$  satisfies (17). We also have that

$$\sigma^P(v, w) = \mathbf{w}^T \Sigma \mathbf{v} = \mathbf{w}^T \mathbf{S}^\dagger \mathbf{v},$$

where  $\mathbf{w}$  and  $\mathbf{v}$  are the vectors collecting the boundary degrees of freedom **(D1)** of two functions  $w$  and  $v$  in  $\mathring{V}_k^h(P)$ . So, we do not actually need to build the basis functions  $\phi_i$ , but we define the action of the bilinear form  $\sigma^P$  directly on the vectors of degrees of freedom. This strategy allows us to reduce the construction of a bilinear form  $\sigma^P(\cdot, \cdot)$  satisfying (17) to the construction of a bilinear form  $\sigma_P^*(\cdot, \cdot)$  satisfying (50).

*Step 4. Factoring out higher order polynomials.* We deal now with the construction of a bilinear form satisfying (50). To this end, we consider the seminorm  $|\cdot|_{-1/2, \partial P} : H^{-\frac{1}{2}}(\partial P) \rightarrow \mathbb{R}^+$  defined by

$$|\eta|_{-1/2, \partial P} = \sup_{\phi \in H_{\mathcal{O}}^{\frac{1}{2}}(\partial P)} \frac{\langle \eta, \phi \rangle}{|\phi|_{1/2, \partial P}}, \quad (52)$$

where the functional space  $H_{\mathcal{O}}^{\frac{1}{2}}(\partial P)$  is defined as

$$H_{\mathcal{O}}^{\frac{1}{2}}(\partial P) = \left\{ v \in H^{\frac{1}{2}}(\partial P) \text{ such that } \int_{\partial P} v = 0 \right\}.$$

Observe that, for all  $\eta \in H^{-\frac{1}{2}}(\partial P)$ , it holds that

$$|\gamma_P^* \eta|_{-1,P} \simeq |\eta|_{-1/2, \partial P}.$$

Then, we can rewrite (50) as

$$\sigma_P^*(\eta, \eta) \simeq |\eta|_{-1/2, \partial P}^2 \quad \text{and} \quad \sigma_P^*(\eta, \mu) \lesssim |\eta|_{-1/2, \partial P} |\mu|_{-1/2, \partial P}. \quad (53)$$

We now split  $N_{k-1}(\partial P)$  as

$$N_{k-1}(\partial P) = N_0(\partial P) \oplus N_0^\perp(\partial P),$$

where  $N_0(\partial P)$  is the space of functions that are constant on each edge of  $\partial P$ , and

$$N_0^\perp(\partial P) = \left\{ \eta \in N_{k-1}(\partial P) : \int_e \eta = 0, \text{ for all edge } e \in \mathcal{E}_P \right\}$$

is the space of piecewise polynomials of order up to  $k-1$  with zero average on each edge of  $\partial P$ . We start by providing a lower bound, which holds for all  $\eta \in N_{k-1}(\partial P)$  under the very weak assumption (G3) on the edge partition  $\mathcal{E}_P$  of  $\partial P$ .

**Lemma 4.6.** *Assume that (G3) holds. Then, for all  $\eta \in N_{k-1}(\partial P)$  with  $\int_{\partial P} \eta = 0$  we have*

$$|\eta|_{-1/2, \partial P}^2 \gtrsim \sum_{e \in \mathcal{E}_P} h_e \int_e |\eta|^2. \quad (54)$$

The proof of this Lemma is quite technical and we report it in Appendix B. On  $N_0^\perp(\partial P)$  we can also prove an upper bound, as stated by the following lemma.

**Lemma 4.7.** *For all  $\eta \in L^2(\partial P)$  such that  $\int_e \eta = 0$  for all edges  $e \in \mathcal{E}_P$ , it holds that*

$$|\eta|_{-1/2, \partial P}^2 \lesssim \sum_{e \in \mathcal{E}_P} h_e \int_e |\eta|^2. \quad (55)$$

*Proof.* Consider  $\eta \in L^2(\partial P)$  such that its average on every edge  $e \in \mathcal{E}_P$  is zero. Let  $v \in H^{\frac{1}{2}}(\partial P)$  and denote its average on  $e$  by  $\bar{v}^e$ . The Cauchy-Schwarz inequality and a Poincaré-like inequality yield

$$\int_e \eta v = \int_e \eta (v - \bar{v}^e) \leq \|\eta\|_{0,e} \|v - \bar{v}^e\|_{0,e} \leq \|\eta\|_{0,e} h_e^{\frac{1}{2}} |v|_{1/2,e},$$

which holds for every edge  $e \in \mathcal{E}_P$ . Using again the Cauchy-Schwarz inequality yields:

$$\begin{aligned} \langle \eta, v \rangle &= \int_{\partial P} \eta v \leq \sum_{e \in \mathcal{E}_P} \|\eta\|_{0,e} h_e^{\frac{1}{2}} |v|_{1/2,e} \leq \left( \sum_{e \in \mathcal{E}_P} h_e \|\eta\|_{0,e}^2 \right)^{\frac{1}{2}} \left( \sum_{e \in \mathcal{E}_P} |v|_{1/2,e}^2 \right)^{\frac{1}{2}} \\ &\lesssim \left( \sum_{e \in \mathcal{E}_P} h_e \|\eta\|_{0,e}^2 \right)^{\frac{1}{2}} |v|_{1/2, \partial P}. \end{aligned}$$

The assertion of the lemma follows by using this inequality in the definition (52) of the seminorm  $|\eta|_{-1/2, \partial P}$ .  $\square$

The following corollary is a straightforward consequence of Lemmas 4.6 and 4.7.

**Corollary 4.8.** *If assumption (G3) holds, then, for all  $\eta \in N_0^\perp(\partial P)$  we have*

$$|\eta|_{-1/2, \partial P}^2 \simeq \sum_{e \in \mathcal{E}_P} h_e \int_e |\eta|^2. \quad (56)$$

Now, every  $\eta \in N_{k-1}(\partial P)$  can be split as  $\eta = \eta^0 + \eta^\perp$  with  $\eta^0 \in N_0(\partial P)$  and  $\eta^\perp \in N_0^\perp(\partial P)$ , and we have

$$\|\eta^\perp\|_{0,e} = \left\| \eta - \int_e \eta \right\|_{0,e} \leq \|\eta\|_{0,e}.$$

Then, using Lemma 4.6 and Lemma 4.7, we can write

$$\begin{aligned} |\eta^\perp|_{-1/2,\partial P}^2 &\lesssim \sum_e h_e \|\eta^\perp\|_{0,e}^2 = \sum_e h_e \left\| \eta - \int_e \eta \pm \int_{\partial P} \eta \right\|_{0,e}^2 \\ &\leq \sum_e h_e \left( \left\| \eta - \int_{\partial P} \eta \right\|_{0,e}^2 + \left\| \int_e (\eta - \int_{\partial P} \eta) \right\|_{0,e}^2 \right) \\ &\lesssim \sum_e h_e \left\| \eta - \int_{\partial P} \eta \right\|_{0,e}^2 \lesssim \left| \eta - \int_{\partial P} \eta \right|_{-1/2,\partial P}^2 = |\eta|_{-1/2,\partial P}^2, \end{aligned}$$

and, by triangular inequality,

$$|\eta^0|_{-1/2,\partial P} \lesssim |\eta|_{-1/2,\partial P} + |\eta^\perp|_{-1/2,\partial P} \lesssim |\eta|_{-1/2,\partial P}.$$

Corollary 4.8 yields the following result.

**Corollary 4.9.** *If assumption (G3) holds, then, for  $\eta \in N_{k-1}(\partial P)$  split as  $\eta = \eta^0 + \eta^\perp$  with  $\eta^0 \in N_0(\partial P)$  and  $\eta^\perp \in N_0^\perp(\partial P)$ , we have*

$$|\eta|_{-1/2,\partial P}^2 \simeq |\eta^0|_{-1/2,\partial P}^2 + |\eta^\perp|_{-1/2,\partial P}^2 \simeq |\eta^0|_{-1/2,\partial P}^2 + \sum_{e \in \mathcal{E}_P} h_e \int_e |\eta - \eta^0|^2.$$

In view of Corollary 4.9, we define the stabilizing bilinear form  $\sigma_P^*(\cdot, \cdot) : N_{k-1}(\partial P) \times N_{k-1}(\partial P) \rightarrow \mathbb{R}$  as

$$\sigma_P^*(\eta, \zeta) = s^0(\eta^0, \zeta^0) + \sum_{e \in \mathcal{E}_P} h_e \int_e (\eta - \eta^0)(\zeta - \zeta^0), \quad (57)$$

where  $s^0(\cdot, \cdot) : N_0(\partial P) \times N_0(\partial P) \rightarrow \mathbb{R}$  can be any bilinear form satisfying

$$s^0(\eta^0, \zeta^0) \lesssim |\eta^0|_{-1/2,\partial P} |\zeta^0|_{-1/2,\partial P}, \quad \text{and} \quad s^0(\eta^0, \eta^0) \gtrsim |\eta^0|_{-1/2,\partial P}^2 \quad (58)$$

for all  $\eta^0, \zeta^0 \in N_0(\partial P)$ . In the next section we will provide three different strategies to build suitable bilinear forms  $s^0(\cdot, \cdot)$ .

## 5. STABILIZATION FOR THE LOWEST ORDER NONCONFORMING VEM

We devote this section to the construction and analysis of several possible bilinear forms  $s^0(\cdot, \cdot) : N_0(\partial P) \times N_0(\partial P) \rightarrow \mathbb{R}$  satisfying (58). We consider three different strategies. The first one is to define  $s^0$  as a weighted  $L^2$  inner product, at the price of the loss of a logarithmic factor in the stability estimate. The second strategy is to resort to the use of a wavelet decomposition of the space  $N_0(\partial P)$ , and take advantage of the equivalent expressions for the Sobolev norms of negative and/or fractionary order that such bases allow. Finally, in the spirit of Remark 3.3, we construct a second, explicitly known, discrete space, in a stable duality relation with  $N_0(\partial P)$ . For this discrete space we explicitly define a bilinear form inducing the  $H^{\frac{1}{2}}(\partial P)$  seminorm, that we use to construct the bilinear form  $s^0(\cdot, \cdot)$  by duality.

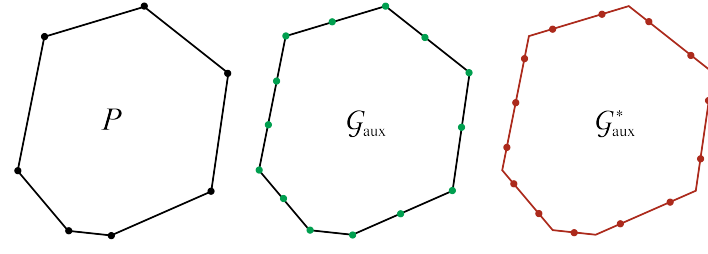


FIGURE 1. A polygon  $P$  (left), the auxiliary quasi-uniform grid  $\mathcal{G}_{\text{aux}}(\partial P)$  (center) and the dual grid  $\mathcal{G}_{\text{aux}}^*(\partial P)$  (right). Remark that the vertices of the polygonal element are not nodes of  $\mathcal{G}_{\text{aux}}^*(\partial P)$ .

**5.1. A quasi optimal stabilization term.** We can define the bilinear form  $s^0$  as

$$s^0(\eta, \mu) = s_{L2}^0(\eta, \mu) = \sum_{e \in \mathcal{E}_P} h_e \int_e \left( \eta - \int_{\partial P} \eta \right) \left( \mu - \int_{\partial P} \mu \right), \quad (59)$$

and we have the following lemma.

**Lemma 5.1.** *If assumption **(G2b)** holds, then, setting*

$$\widehat{h}_P = \min_{e \in \mathcal{E}_P} h_e,$$

for all  $\eta \in N_0(\partial P)$  we have

$$(1 + \log(h_P/\widehat{h}_P))^{-1} |\eta|_{-1/2, \partial P}^2 \lesssim s^0(\eta, \eta) \lesssim |\eta|_{-1/2, \partial P}^2.$$

*Proof.* Thanks to Lemma 4.6, we only need to prove the first inequality. We consider an auxiliary quasi-uniform mesh  $\mathcal{G}_{\text{aux}}(\partial P)$  on  $\partial P$  with mesh size  $\widehat{h}_P$  containing, as nodes, all the vertices of  $P$ , and we let  $\mathcal{G}_{\text{aux}}^*(\partial P)$  denote the dual mesh of  $\mathcal{G}_{\text{aux}}(\partial P)$ , whose nodes are the midpoints of the elements of  $\mathcal{G}_{\text{aux}}(\partial P)$  (see Figure 1).

Then, we let  $N_{\text{aux}}(\partial P)$  and  $N_{\text{aux}}^*(\partial P)$  denote, respectively, the space of piecewise constant functions on the mesh  $\mathcal{G}_{\text{aux}}(\partial P)$ , and the space of average free continuous piecewise linear functions on the mesh  $\mathcal{G}_{\text{aux}}^*(\partial P)$ . Observe that  $N_0(\partial P) \subseteq N_{\text{aux}}(\partial P)$ . We know (cf. [62], see also Corollary 5.5 in the following) that for  $\eta \in N_0(\partial P)$  it holds that

$$|\eta|_{-1/2, \partial P} \lesssim \sup_{v \in N_{\text{aux}}^*(\partial P)} \frac{\int_{\partial P} \eta v}{|v|_{1/2, \partial P}}. \quad (60)$$

Now, for  $\eta \in N_0(\partial P)$  and  $v \in N_{\text{aux}}^*(\partial P)$ , applying the Cauchy-Schwartz inequality twice, we obtain:

$$\begin{aligned} \int_{\partial P} \eta v &\lesssim \|v\|_{L^\infty(\partial P)} \int_{\partial P} |\eta| = \|v\|_{L^\infty(\partial P)} \sum_{e \in \mathcal{E}_P} \int_e |\eta| \\ &\lesssim \|v\|_{L^\infty(\partial P)} \sqrt{\#(\mathcal{E}_P)} \sqrt{\sum_{e \in \mathcal{E}_P} \left( \int_e |\eta| \right)^2} \lesssim \|v\|_{L^\infty(\partial P)} \sqrt{\sum_{e \in \mathcal{E}_P} h_e \int_e |\eta|^2}. \end{aligned}$$

Therefore, plugging this last bound into (60), we obtain, for every  $\eta \in N_0(\partial P) \subseteq N_{\text{aux}}(\partial P)$ ,

$$|\eta|_{-1/2, \partial P} \lesssim \sup_{v \in N_{\text{aux}}^*} \frac{\|v\|_{L^\infty(\partial P)}}{|v|_{1/2, \partial P}} \sqrt{\sum_{e \in \mathcal{E}_P} h_e \int_e |\eta|^2}.$$

It remains to bound the  $L^\infty(\partial P)$  norm of  $v$  in terms of its  $H^{\frac{1}{2}}(\partial P)$  seminorm. To this aim, we use an inverse inequality on the space of continuous piecewise linear polynomials  $N_{\text{aux}}^*(\partial P)$ , cf. [19, Lemma 3.2(i)], and obtain

$$|\eta|_{-1/2, \partial P} \lesssim \sqrt{1 + \log(h_P/\hat{h}_P)} \left( \sum_{e \in \mathcal{E}_P} h_e \int_e |\eta|^2 \right)^{1/2} = \sqrt{1 + \log(h_P/\hat{h}_P)} \left( \sum_{e \in \mathcal{E}_P} h_e \|\eta\|_{0,e}^2 \right)^{1/2}. \quad (61)$$

Remarking that

$$|\eta|_{-1/2, \partial P} = \left| \eta - \int_{\partial P} \eta \right|_{-1/2, \partial P}$$

concludes the proof.  $\square$

If we now use the bilinear form  $s^0$  defined above in the design of the stabilization bilinear form for the space  $V_k^h(P)$ , we have that (17) is satisfied possibly with the loss of a logarithmic factor if assumption **(G2a)** is violated, as stated by the following corollary.

**Corollary 5.2.** *Let assumption **(G2b)** hold, and let  $\sigma_P^*$  be defined by (57) with  $s^0$  defined by (59). Then, the dual bilinear form  $\sigma^P : V_k^h(P) \times V_k^h(P) \rightarrow \mathbb{R}$  defined by (51) verifies, for all  $v, w \in V_k^h(P) \cap \ker(\Pi_k^{\nabla, P})$*

$$a^P(v, v) \lesssim \sigma^P(v, v) \lesssim (1 + \log(h_P/\hat{h}_P)) a^P(v, v).$$

**5.2. An optimal stabilization based on a wavelet decomposition.** In order to define a bilinear form  $s^0(\cdot, \cdot)$  satisfying (50) on  $N_0(\partial P)$ , we can exploit some known norm equivalences for the space  $H^{-\frac{1}{2}}(\partial P)$ , based on wavelet decompositions. On a circle  $\widehat{\Gamma}$  of unitary length, we consider the increasing sequence of spaces  $\{V_j\}_{j=0}^\infty$ , where  $V_j \subset L^2(\widehat{\Gamma})$  is the space of piecewise constant functions on the uniform grid on  $\widehat{\Gamma}$  with mesh size  $2^{-j}$ . Let  $\{s_k^j\}_{k=0}^{2^j-1}$  denote the nodes of the corresponding mesh, which we assume to be ordered counter-clockwise. As  $V_j \subset V_{j+1}$ , for all level  $j$  we can decompose  $\eta_{j+1} \in V_{j+1}$  as  $\eta_{j+1} = \eta_j + \delta_j$ , with  $\eta_j \in V_j$  obtained by applying a suitable oblique projector  $Q_j$  to  $\eta_{j+1}$ . For a given  $M > 0$ , this gives us a telescopic expansion of all function in  $V_M$  as  $\eta_M = \eta_0 + \sum_{j=0}^{M-1} \delta_j$ , and, passing to the limit as  $M$  goes to infinity, of all functions  $\eta$  in  $L^2(\widehat{\Gamma})$  as  $\eta = \eta_0 + \sum_{j=0}^\infty \delta_j$ . For  $\eta \in L^2(\widehat{\Gamma})$ , we can introduce the vector  $\kappa_j(\eta)$  of length  $2^j$ , that uniquely determines  $Q_j\eta$ :

$$\kappa_j(\eta) := \{\kappa_{jk}\}_{k=0}^{2^j-1} \quad \text{with} \quad \kappa_{jk} = 2^{j/2} \int_{s_k^j}^{s_{k+1}^j} Q_j \eta.$$

As  $Q_j$ , whose precise definition is out of the scope of this paper, is a projector, for  $\eta \in V_j$  we have  $Q_j\eta = \eta$  and hence, in such a case,  $\kappa_{jk} = \int_{s_k^j}^{s_{k+1}^j} \eta$ .

Let  $\delta_j(\eta)$  be the vector of coefficients of  $\delta_j = (Q_{j+1} - Q_j)\eta$  with respect to a suitable basis for the space  $W_j = (1 - Q_j)V_{j+1}$ , whose definition is also out of the scope of this paper (see [39] for more details). Given  $\kappa_{j+1}(\eta)$ , we compute  $\kappa_j(\eta) := \{\kappa_{jk}\}_{k=0}^{2^j-1}$  by subsampled convolution with a *low-pass filter*  $h$  of length  $L + 1$ , which is strictly related with the projector  $Q_j$ , and  $\delta_j(\eta) := \{\delta_{jk}\}_{k=0}^{2^j-1}$  by subsampled convolution with the *band-pass filter*  $g = [1, -1]$ . More precisely, we have

$$\kappa_{jk} = \sum_{l=0}^L \frac{\sqrt{2}}{2} h(l) \kappa_{j+1,2k+l} \quad \text{and} \quad \delta_{jk} = \sum_{l=0}^1 \frac{\sqrt{2}}{2} g(l) \kappa_{j+1,2k+l} = \frac{\sqrt{2}}{2} (\kappa_{j+1,2k} - \kappa_{j+1,2k+1}).$$

In the above computations, the function  $\eta$  is considered as periodic, so that we extend the vector  $\kappa_{j+1}(\eta)$  as  $\kappa_{j+1,2^{j+1}+k} = \kappa_{j+1,k}$ ,  $k \geq 0$ , when  $2k + l > 2^{j+1} - 1$ . For suitable choices of the low pass filter  $h$ , the following norm equivalence holds for all  $\eta \in H^{-\frac{1}{2}}(\widehat{\Gamma})$  (see [40])

$$|\eta|_{-1/2,\widehat{\Gamma}}^2 \simeq \sum_{j=0}^{\infty} 2^{-j} \|\delta_j(\eta)\|_2^2,$$

where  $\|\cdot\|_2$  denotes the Euclidean norm. There are several possible choices for the oblique projector  $Q_j$  and the relative low pass filter  $h$  (see [39]). In our experiments, we choose the so called (2,2)-*biorthogonal wavelet*, cf. [39], for which the low pass filter  $h$  is

$$h = \frac{\sqrt{2}}{2} \left[ \frac{3}{128}, -\frac{3}{128}, -\frac{11}{64}, \frac{11}{64}, 1, 1, \frac{11}{64}, -\frac{11}{64}, -\frac{3}{128}, \frac{3}{128} \right].$$

In order to exploit such a norm equivalence, we embed the grid on  $\partial P$ , whose elements are the edges of  $P$ , in a quasi uniform mesh  $\mathcal{G}_{\text{aux}}$  with  $2^M$  elements, where  $M$  is the smallest integer such that  $M > \log_2(\sum_{e \in \mathcal{E}_P} h_e / (\min_{e \in \mathcal{E}_P} h_e))$ .

We then consider a continuous piecewise linear (in the curvilinear abscissas) mapping  $\Theta : \widehat{\Gamma} \rightarrow \partial P$ , such that the nodes of the uniform dyadic grid of  $\widehat{\Gamma}$  with  $2^M$  elements are mapped to the nodes of  $\mathcal{G}_{\text{aux}}$ . A change of variable argument yields the scaling relation

$$|\eta|_{-1/2,\partial P} \simeq h_P |\eta \circ \Theta|_{-1/2,\widehat{\Gamma}}.$$

Then, for  $\eta, \mu \in N_0(\partial P)$ , we define

$$s^0(\eta, \mu) = s_{\text{wav}}^0(\eta, \mu) = h_P^2 \sum_{j=0}^M 2^{-j} \delta_j(\eta \circ \Theta)^T \delta_j(\mu \circ \Theta)^T. \quad (62)$$

The vectors  $\delta_j(\eta \circ \Theta)$  and  $\delta_j(\mu \circ \Theta)$  can be computed efficiently by a *fast wavelet transform*. We have the following corollary.

**Corollary 5.3.** *Let assumption (G3) hold, and let  $\sigma_P^*$  be defined by (57) with  $s^0$  defined by (62). Then, the dual bilinear form  $\sigma^P : V_k^h(P) \times V_k^h(P) \rightarrow \mathbb{R}$  defined by (51) verifies, for all  $v, w \in V_k^h(P) \cap \ker(\Pi_k^{\nabla, P})$ ,*

$$a^P(v, v) \lesssim \sigma^P(v, v) \lesssim a^P(v, v).$$

**5.3. An optimal stabilization based on a known dual space.** In the spirit of Remark 3.3, we can look at  $N_0(\partial P)$  as the stable dual space of a third, explicitly known space  $\tilde{N}_0(\partial P) \subset H^{\frac{1}{2}}(\partial P)$ . Then, we can construct an optimal stabilizing form  $s^0$  on  $N_0(\partial P)$  if we are able to construct a bilinear form on  $\tilde{N}_0(\partial P)$  that is spectrally equivalent to the  $H^{\frac{1}{2}}(\partial P)$  semi-inner product. A key ingredient in the construction is an oblique projector onto the continuous piecewise linears, studied by Steinbach in [62].

Let  $\mathcal{G}$  and  $\mathcal{G}^*$  denote, respectively, a grid on  $\partial P$ , and the dual grid, whose nodes are the midpoints of the elements of  $\mathcal{G}$ . We let  $K(\mathcal{G})$  and  $\tilde{K}(\mathcal{G}^*)$  denote the space of piecewise constant functions on  $\mathcal{G}$  and space of continuous linear functions on  $\mathcal{G}^*$ . We can define the projector  $\tilde{Q} : L^2(\partial P) \rightarrow \tilde{K}(\mathcal{G}^*)$  as

$$\langle \tilde{Q}v - v, w_h \rangle = 0 \quad \forall w_h \in K(\mathcal{G}).$$

The following theorem holds.

**Theorem 5.4.** *Assume that there exists a constant  $c' \geq 1$  such that for any two adjacent intervals  $e$  and  $e'$  in  $\mathcal{G}$  it holds that*

$$\frac{h_e}{h_{e'}} \leq c'.$$

*Then, if  $c' < c_0 \approx 3.672688104237926$ , the projector  $\tilde{Q}_h$  is bounded in  $H^{\frac{1}{2}}(\partial P)$ :*

$$\|\tilde{Q}v\|_{-1/2, \partial P} \lesssim \|v\|_{1/2, \partial P},$$

*the implicit constant in the inequality depending on  $c'$ .*

The proof of Theorem 5.4, which also yields the value of the constant  $c_0$ , is the same as the proof of the analogous result in [62, Theorem 4.3 and Section 5], where the roles of the grids  $\mathcal{G}$  and  $\mathcal{G}^*$  are, however, switched. Nevertheless, the arguments therein apply unchanged to the present case, though resulting in a different value of  $c_0$ , as detailed in Appendix C. Using  $\tilde{Q}_h$  as a Fortin projector, we find the result stated in the following corollary.

**Corollary 5.5.** *Under the assumptions of Theorem 5.4, the following inf-sup conditions hold:*

$$\inf_{w \in K(\mathcal{G})} \sup_{v \in \tilde{K}(\mathcal{G}^*)} \frac{\int_{\partial P} wv}{\|v\|_{1/2, \partial P} \|w\|_{-1/2, \partial P}} \gtrsim 1, \quad \inf_{v \in \tilde{K}(\mathcal{G}^*)} \sup_{w \in K(\mathcal{G})} \frac{\int_{\partial P} wv}{\|v\|_{1/2, \partial P} \|w\|_{-1/2, \partial P}} \gtrsim 1.$$

Assume now that the tessellation satisfies Assumption **(G2a)** with a constant  $\gamma_2 < c_0$ , where  $c_0$  is given in Theorem 5.4. We let  $\tilde{N}_0(\partial P)$  denote the space of piecewise linear (in the arclength ascissa on the boundary) functions on the grid  $\mathcal{G}^*$  whose nodes are the midpoints of the edges of  $P$ . Corollary 5.5 implies the inf-sup condition

$$\inf_{\eta \in N_0(\partial P)} \sup_{\phi \in \tilde{N}_0(\partial P)} \frac{\int_{\partial P} \lambda \phi}{\|\lambda\|_{-1/2, \partial P} \|\phi\|_{1/2, \partial P}} \gtrsim 1.$$

Once again, we resort to the duality technique presented in Section 3 by setting, this time,

- $V = H^{\frac{1}{2}}(\partial P)$ ,  $V' = H^{-\frac{1}{2}}(\partial P)$ ,
- $W = \tilde{N}_0(\partial P)$ ,  $W^* = N_0(\partial P)$ ,
- $\widehat{W} = \widehat{W}^* = \mathbb{P}_0(\partial P)$ .

We take the projection  $\hat{\Pi}$  as the  $L^2(\partial P)$ -orthogonal projection onto the constants. We need to define a bilinear form  $\tilde{\sigma}^P$  on the known space  $\tilde{N}_0(\partial P)$  satisfying

$$\tilde{\sigma}^P(\phi, \phi) \simeq |\phi|_{1/2, \partial P}^2, \quad \tilde{\sigma}^P(\phi, \psi) \lesssim |\phi|_{1/2, \partial P} |\psi|_{1/2, \partial P}. \quad (63)$$

The problem of defining bilinear forms satisfying (63) on the space of continuous piecewise linear functions has been addressed in other numerical frameworks, such as, for example, the one of domain decomposition methods (see, for instance, [26]) or the stabilization of the conforming VEM method (see [13]). We will present two possible options at the end of this Section.

Assume now to have such a bilinear form. Let  $\mathfrak{B}_0 = \{\zeta_0^e, e \in \mathcal{E}_P\}$ , with  $\zeta_0^e$  denoting the characteristic function of the edge  $e$ , denote the natural basis for  $N_0(\partial P)$ , and  $\tilde{\mathfrak{B}}_0 = \{\tilde{\phi}_{e_i}, i = 1, \dots, \#\mathcal{E}_P\}$  be the basis for  $\tilde{N}_0(\partial P)$ , dual to  $\mathfrak{B}_0$ , that is,  $\tilde{\phi}_{e_i}$  is the unique piecewise linear function on the dual grid  $\mathcal{G}^*$  such that

$$\int_{\partial P} \tilde{\phi}_{e_i} \zeta_0^{e_j} = \int_{e_j} \tilde{\phi}_{e_i} = \delta_{i,j}, \quad j = 1, \dots, \#\mathcal{E}_P.$$

We define the relative stiffness matrix

$$\tilde{\Sigma} = (\tilde{\sigma}_{i,j}), \quad \tilde{\sigma}_{i,j} = \tilde{\sigma}^P(\tilde{\phi}_{e_i}, \tilde{\phi}_{e_j}).$$

Let  $S_0 = \tilde{\Sigma}^\dagger = (s_{i,j}^0)$ . We can define  $s^0 : N_0(\partial P) \times N_0(\partial P) \rightarrow \mathbb{R}$  by setting

$$s^0(\zeta_{e_i}, \zeta_{e_j}) = s_{i,j}^0, \quad i, j = 1, \dots, \#\mathcal{E}_P. \quad (64)$$

Proposition 3.2 yields, for all  $\eta \in N_0(\partial P)$

$$s^0(\eta, \eta) \simeq |\eta|_{-1/2, \partial P}^2.$$

We have the following corollary.

**Corollary 5.6.** *Let assumption **(G2a)** hold with  $\gamma_2 < c_0$ ,  $c_0$  given by Theorem 5.4, and let  $\sigma_P^*$  be defined by (57) with  $s^0$  defined by (64). Then, the dual bilinear form  $\sigma^P : V_k^h(P) \times V_k^h(P) \rightarrow \mathbb{R}$  defined by (51) verifies, for all  $v, w \in V_k^h(P) \cap \ker(\Pi_k^{\nabla, P})$*

$$a^P(v, v) \lesssim \sigma^P(v, v) \lesssim a^P(v, v).$$

As observed in Remark 3.3, we find that  $S_0^\dagger = \tilde{\Sigma}^{\dagger\dagger} = \tilde{\Sigma}$ , and, consequently, the bilinear form  $\sigma^P$  mentioned in the above corollary, takes the form

$$\sigma^P(u, v) = \sum_{i,j=1}^{\#\mathcal{E}_P} \tilde{\sigma}_{i,j} \langle \zeta_0^{e_i}, u \rangle \langle \zeta_0^{e_j}, v \rangle + \sum_e h_e^{-1} \int_e \pi_{\partial P}^0 u \pi_{\partial P}^0 v.$$

**Remark 5.7.** Analogously to what we proposed in Section 5.2, if the tessellation does not satisfy the gradedness Assumption **(G2a)** with  $\gamma_2 < c_0$ , it is always possible to embed the mesh induced on  $\partial P$  by the vertexes of  $P$  in a finer mesh satisfying the assumptions of Theorem 5.4. Then, we can define  $\sigma_P^*$  on the space of piecewise constants on such a finer grid and then restrict it to  $N_0(\partial P)$ . In such a case, the finer mesh is only needed for the computation of low order component of the stabilization bilinear form.

We conclude this section by recalling two possibilities for the definition of the bilinear form  $\tilde{\sigma}^P$ . We let

$$b(u, w) = \int_{\partial P} u' v',$$

denote the bilinear form relative to the Laplace-Beltrami operator on  $\partial P$ , with  $\tilde{R} = (r_{i,j})$ ,  $r_{i,j} = b(\tilde{\phi}_{e_i}, \tilde{\phi}_{e_j})$ , being the stiffness matrix relative to its Galerkin discretization, and  $\tilde{M} = (m_{i,j})$ ,  $m_{i,j} = \int_{\partial P} \tilde{\phi}_{e_i} \tilde{\phi}_{e_j}$  the corresponding mass matrix. The first possibility is to define  $\tilde{\sigma}^P$  as the scaled Laplace-Beltrami operator, which corresponds to setting

$$\tilde{\Sigma} = h_P \tilde{R}.$$

This bilinear form has been proposed in [13] as a stabilization for the conforming virtual element methods, where the traces of virtual functions on the boundary of the elements are continuous piecewise linear polynomials. We let  $s_{\text{SLB}}^0 : N_0(\partial P) \times N_0(\partial P) \rightarrow \mathbb{R}$  denote the bilinear form resulting from such a choice.

The second possibility, originally proposed in the domain decomposition framework (cf. [26] and [24, page 1110]), is to define  $\tilde{\sigma}^P$  as the square root of the Laplace-Beltrami operator, which correspond to setting

$$\tilde{\Sigma} = \tilde{M}^{1/2} (\tilde{M}^{-1/2} \tilde{R} \tilde{M}^{-1/2})^{1/2} \tilde{M}^{1/2}.$$

Remark that if the grid  $\mathcal{G}^*$  is quasi-uniform, then, using mass lumping, the contributes of the mass matrix  $\tilde{M}$  cancel out and the above definition reduces to  $\tilde{\Sigma} = \tilde{R}^{1/2}$ . We let  $s_{\text{rLB}}^0 : N_0(\partial P) \times N_0(\partial P) \rightarrow \mathbb{R}$  denote the bilinear form resulting from such a choice.

## 6. IMPLEMENTATION AND NUMERICAL EXPERIMENTS

**6.1. Construction of the stabilizing bilinear form.** Before presenting the numerical tests, we give some detail on the algebraic realization of the bilinear form  $\sigma^P(\cdot, \cdot)$ .

For convenience of exposition, we introduce a local numbering of the elemental edges, e.g., we denote the  $\ell$ -th edge in  $\mathcal{E}_P$  by  $e_\ell$  with subindex  $\ell$  running from 1 to  $N = \#\mathcal{E}_P$ , the cardinality of the edge set  $\mathcal{E}_P$ . We select the boundary degrees of freedom (**D1**) on each edge of  $\partial P$  so that  $\mathfrak{B}$  contains the subset  $\mathfrak{B}_0 = \{\zeta_0^{e_\ell}, \ell = 1, \dots, N\}$ , forming a basis of  $N_0(\partial P)$ , with the remaining basis functions having zero average on the elemental edges. The basis  $\mathfrak{B}$  will then have the form  $\mathfrak{B} = \mathfrak{B}_0 \cup \{\zeta_i^{e_\ell}, \ell = 1, \dots, N, i = 1, \dots, k-1\}$ , where, for  $\ell = 1, \dots, N$ , the set  $\{\zeta_i^{e_\ell}, i = 1, \dots, k-1\}$  is a basis for the space of average free polynomials of order at most  $k-1$  on  $e_\ell$ .

Let  $S_0 = (s_{\ell,\ell'})$  be the matrix having coefficients  $s_{\ell,\ell'} = s^0(\zeta_0^{e_\ell}, \zeta_0^{e_{\ell'}})$ . This choice of the basis implies that matrix  $S$  is block diagonal up to a permutation of its rows and columns, which corresponds to a suitable renumbering of the edge basis functions, and takes the form

$$S = \begin{pmatrix} S_0 & \mathbf{0} & \cdots & \mathbf{0} \\ \mathbf{0} & h_{e_1} M_1 & \cdots & \mathbf{0} \\ \vdots & \vdots & \ddots & \vdots \\ \mathbf{0} & \mathbf{0} & \cdots & h_{e_N} M_N \end{pmatrix},$$

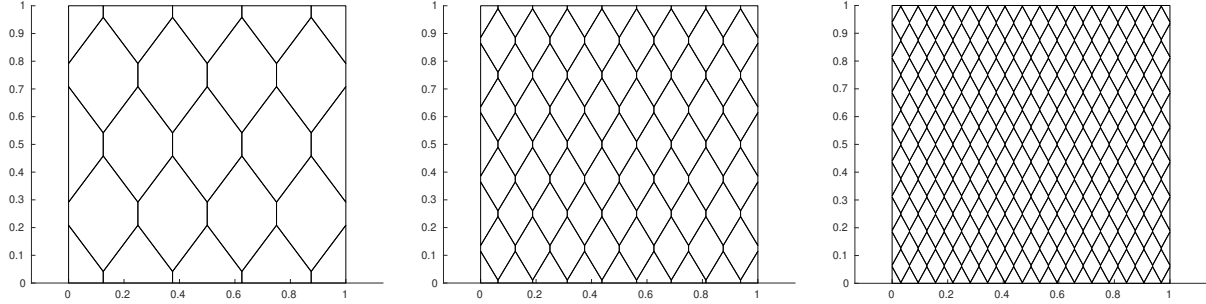


FIGURE 2. Test Case 1: Mesh family  $\mathcal{M}_1$  (hexagonal elements with progressively collapsing edges)

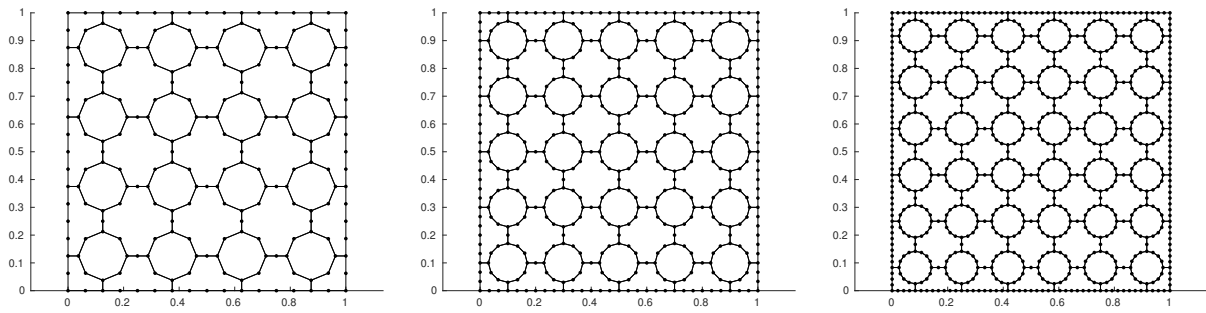


FIGURE 3. Test Case 2: Mesh family  $\mathcal{M}_2$  (polygonal elements with an increasing number of edges)

where  $\mathbf{M}_\ell$  is the mass matrix for the space of average free polynomials of order at most  $k-1$  on the edge  $e_\ell$ , which is given by the edge integral

$$\mathbf{M}_\ell|_{i,j} = \int_{e_\ell} \zeta_i^{e_\ell} \zeta_j^{e_\ell} \quad i, j = 1, \dots, k-1.$$

As the matrices  $\mathbf{M}_\ell$  are nonsingular, it is not difficult to check that the reflexive generalized inverse  $\mathbf{S}^\dagger$  of  $\mathbf{S}$ , as defined in Section 3, has a block diagonal structure and it is given by

$$\mathbf{S}^\dagger = \begin{pmatrix} \mathbf{S}_0^\dagger & \mathbf{0} & \cdots & \mathbf{0} \\ \mathbf{0} & h_{e_1}^{-1} \mathbf{M}_1^{-1} & \cdots & \mathbf{0} \\ \vdots & \vdots & \ddots & \vdots \\ \mathbf{0} & \mathbf{0} & \cdots & h_{e_N}^{-1} \mathbf{M}_N^{-1} \end{pmatrix}.$$

**6.2. Numerical tests.** The main goal of this section is to assess the effectiveness of the virtual element method with the stabilization forms proposed in the previous sections. In particular, we want to investigate experimentally the robustness of the approximation when using sequence of meshes with possibly unbounded number of edges per element, and possibly very small edges adjacent to large edges. We recall that such kind of mesh sequences violate the mesh regularity assumption **(G2)**, although they may satisfy the relaxed condition **(G2a)** or **(G2b)**, and the weaker assumption **(G3)**. To this end, we compare the accuracy of *five* different numerical approximations (6) obtained by using these stabilizations in the practical implementation of the VEM:

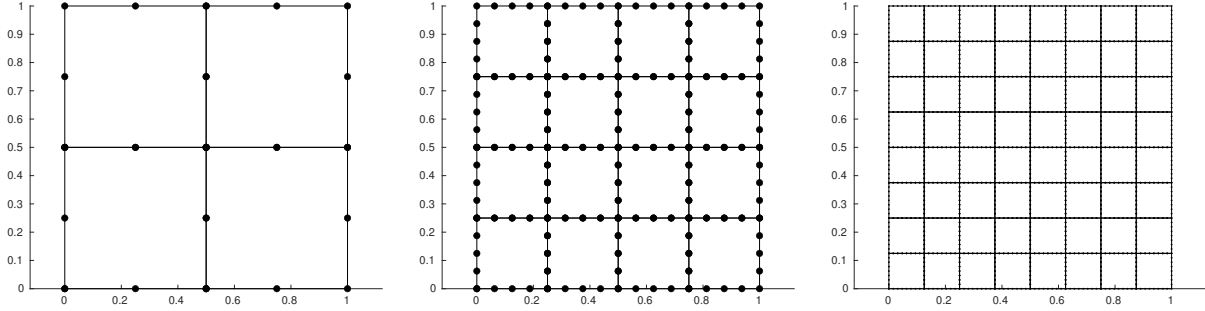


FIGURE 4. Test Case 3: Mesh family  $\mathcal{M}_3$  (polygonal elements with a number of edges that doubles at each refinement)

- $\sigma_1$ : standard choice as proposed in [7];
- $\sigma_i, i = 2, 3, 4, 5$  obtained by duality with  $\sigma_i^*$  defined by (57) with the following choices for the bilinear form  $s^0$ :
  - $\sigma_2$ :  $s^0 = s_{L2}^0$  (weighted  $L^2$  scalar product);
  - $\sigma_3$ :  $s^0 = s_{sLB}^0$  (scaled Laplace–Beltrami operator);
  - $\sigma_4$ :  $s^0 = s_{rLB}^0$  (square root of the Laplace–Beltrami operator).
  - $\sigma_5$ :  $s^0 = s_{wav}^0$  (wavelet bases equivalent norm);

We solve Poisson problem (6) on the computational domain  $\Omega = (0, 1) \times (0, 1)$  after setting the load term  $f$  and nonhomogeneous Dirichlet boundary conditions  $g$  on the domain boundary  $\Gamma$  in accordance with the exact solution:

$$u(x, y) = \frac{1}{2\pi^2} \cos(\pi x) \cos(\pi y). \quad (65)$$

All tests are performed using the enhanced non conforming virtual element discretization space  $V_k^{h,\text{en}}(P)$ , and setting  $f_h = \Pi_k^0 f$ , where  $\Pi_k^0 : L^2(\Omega) \rightarrow \mathbb{P}_k(\Omega_h)$  is the  $L^2$  orthogonal projection onto the space of discontinuous piecewise polynomials of order up to  $k$  on  $\Omega_h$ . In all our implementations, we use orthogonal polynomials as the basis in  $\mathbb{P}_k(P)$  for every  $P \in \Omega_h$  and  $\mathbb{P}_k(e)$  for every  $e \in \mathcal{E}$  (see Remark 2.1). The linear system assembled in any implementation of the VEM is solved by applying the direct solver `PaStiX` [49].

We run our numerical calculations on three different mesh families:

- $\mathcal{M}_1$ : meshes of hexagonal elements with progressively collapsing edges, see Figure 2;
- $\mathcal{M}_2$ : meshes of polygonal elements with an increasing number of edges, see Figure 3;
- $\mathcal{M}_3$ : meshes of polygonal elements with a square boundary  $\partial P$  partitioned in a number of edges that doubles at each refinement, see Figure 4.

Three meshes of each family are shown in Figures 2, 3, and 4. For each mesh, we provide the following data:  $N_{\text{el}}$ , the number of elements of  $\Omega_h$ ;  $N_{\text{ed}}$ , the number of edges of  $\mathcal{E}$ ;  $h = \max_{P \in \Omega_h} h_P$ , the mesh size coefficient;  $\hat{h} = \min_{e \in \mathcal{E}} h_e$ , length of the smallest edge,  $\gamma_h = \max_{P \in \Omega_h} (h_P / \hat{h}_P)$ , largest ratio element diameter/smallest edge, where, we recall  $\hat{h}_P = \min_{e \in \mathcal{E}_P} h_e$ . All mesh families satisfy Assumption **(G1)** and **(G3)**. The family  $\mathcal{M}_1$  does not satisfy Assumption **(G2a)**, while the families  $\mathcal{M}_2$  and  $\mathcal{M}_3$  do not satisfy Assumption **(G2b)**.

Mesh	$N_{\text{el}}$	$N_{\text{ed}}$	$h$	$\hat{h}$	$\gamma_h$
1	77	232	$2.08 \cdot 10^{-1}$	$2.08 \cdot 10^{-2}$	6.08
2	281	844	$1.15 \cdot 10^{-1}$	$5.21 \cdot 10^{-3}$	$1.25 \cdot 10^1$
3	1073	3220	$5.99 \cdot 10^{-2}$	$1.30 \cdot 10^{-3}$	$2.59 \cdot 10^1$
4	4193	12 580	$3.06 \cdot 10^{-2}$	$3.26 \cdot 10^{-4}$	$5.28 \cdot 10^1$

TABLE 1. Test Case 1: data of mesh family  $\mathcal{M}_{1A}$  (shrinking factor = 1/2).

Mesh	$N_{\text{el}}$	$N_{\text{ed}}$	$h$	$\hat{h}$	$\gamma_h$
1	77	232	$2.08 \cdot 10^{-1}$	$2.08 \cdot 10^{-2}$	6.08
2	281	844	$1.25 \cdot 10^{-1}$	$8.14 \cdot 10^{-5}$	$8.58 \cdot 10^2$
3	1073	3220	$6.25 \cdot 10^{-2}$	$3.18 \cdot 10^{-7}$	$1.10 \cdot 10^5$
4	4193	12 580	$3.13 \cdot 10^{-2}$	$1.24 \cdot 10^{-9}$	$1.41 \cdot 10^7$

TABLE 2. Test Case 1: data of mesh family  $\mathcal{M}_{1B}$  (shrinking factor = 1/128).

We test the convergence of the VEM by computing the relative approximation errors defined as:

$$e_0^u = \frac{\|u - \Pi_k^0 u\|_{0,\Omega}}{\|u\|_{0,\Omega}} \quad \text{and} \quad e_1^u = \frac{\|\nabla u - \Pi_{k-1}^0 \nabla u\|_{0,\Omega}}{\|\nabla u\|_{0,\Omega}}$$

for  $k = 1, 2, 3, 4$ .

*Test Case 1.* In Test Case 1, we apply the VEM to the family of hexagonal meshes with collapsing edges shown in Fig. 2. We want to investigate the robustness of the different stabilizations  $\sigma_i$ ,  $i = 1, 2, 3, 4$ , with respect to the rate at which  $\gamma_h$  grows. To this end, at each refinement step we shrink the minimum edge length by a *shrinking factor* so that  $\hat{h}_P$  decreases faster than the mesh size factor  $h_P$ . In practice, we consider two different families of refined meshes, e.g.,  $\mathcal{M}_{1A}$  and  $\mathcal{M}_{1B}$ , with a shrinking factor for the minimum edge length equal to 1/2 and 1/128, respectively. We report the data for these meshes in Tables 1 and 2.

Figures 5, 6 show the convergence plots of  $e_0^u$  and  $e_1^u$ . As expected, the errors  $e_0^u$  and  $e_1^u$  behave like  $\mathcal{O}(h^{k+1})$  and  $\mathcal{O}(h^k)$ , respectively. All the stabilization strategies exhibit similar performance. When  $k = 1$ , as far as  $e_0^u$  is concerned, the stabilizations  $\sigma_1$  and  $\sigma_2$  exhibit a slightly more favorable error constant with respect to  $\sigma_3$  and  $\sigma_4$ . When  $k = 4$ , as far as  $e_1^u$  is concerned, the  $\sigma_1$  stabilization does not perform as well as the other ones.

Mesh	$N_{\text{el}}$	$N_{\text{ed}}$	$h$	$\hat{h}$	$\gamma_h$
1	41	448	$2.61 \cdot 10^{-1}$	$3.13 \cdot 10^{-2}$	8.09
2	145	2368	$1.31 \cdot 10^{-1}$	$9.38 \cdot 10^{-3}$	$1.39 \cdot 10^1$
3	545	11 136	$6.53 \cdot 10^{-2}$	$4.29 \cdot 10^{-3}$	$1.52 \cdot 10^1$
4	2113	55 552	$3.26 \cdot 10^{-2}$	$1.56 \cdot 10^{-3}$	$2.09 \cdot 10^1$

TABLE 3. Test Case 2: data of mesh family  $\mathcal{M}_{2A}$ .

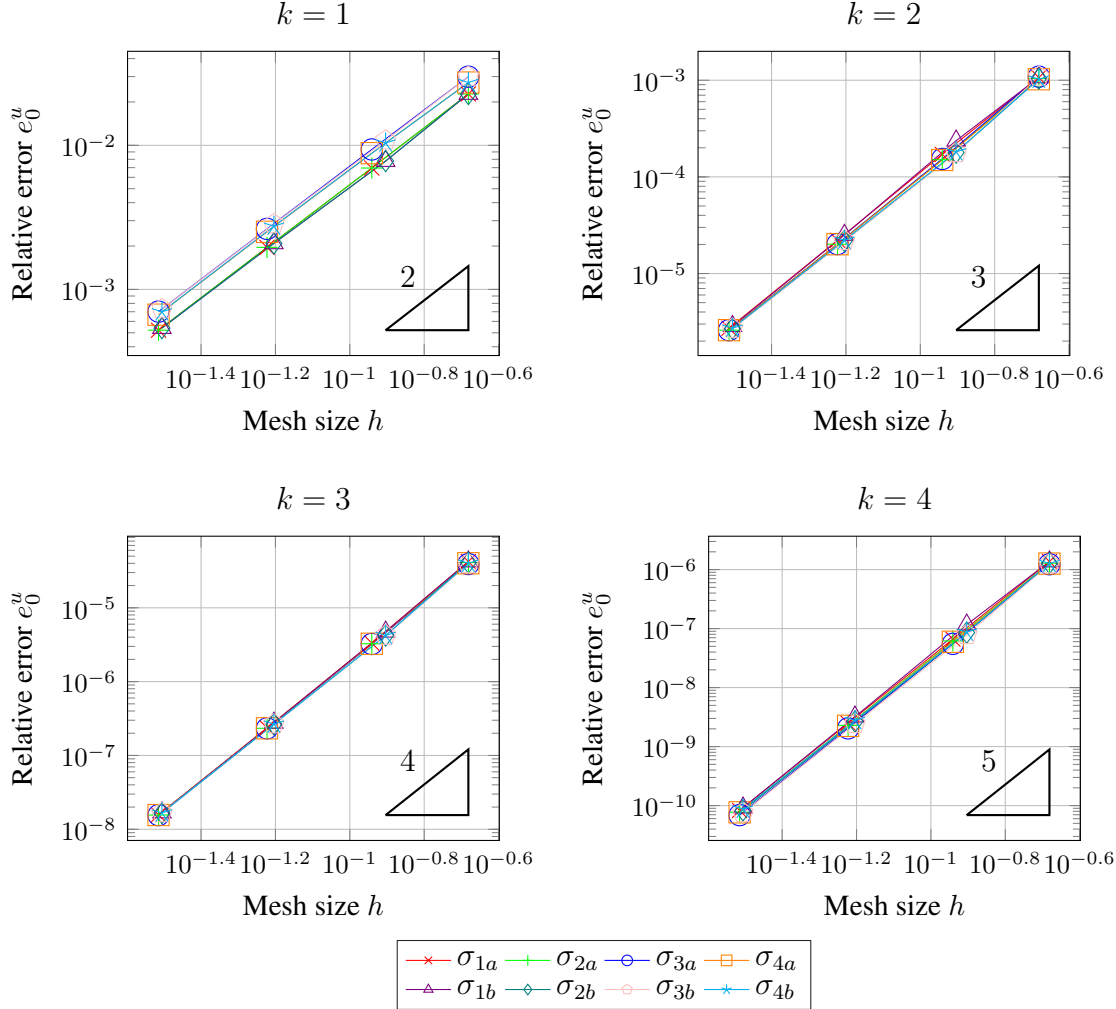


FIGURE 5. Test Case 1: convergence plots for  $e_0^u$  using the hexagonal meshes  $\mathcal{M}_{1A}$  and  $\mathcal{M}_{1B}$ , and the four stabilization strategies  $\sigma_i$ ,  $i = 1, 2, 3, 4$ . Top row: plots for  $k = 1$  (left panel) and  $k = 2$  (right panel); bottom row: plots for  $k = 3$  (left panel) and  $k = 4$  (right panel).

Mesh	$N_{\text{el}}$	$N_{\text{ed}}$	$h$	$\hat{h}$	$\gamma_h$
1	41	448	$2.61 \cdot 10^{-1}$	$3.13 \cdot 10^{-2}$	8.09
2	145	3008	$1.31 \cdot 10^{-1}$	$8.58 \cdot 10^{-3}$	$1.52 \cdot 10^1$
3	545	22 400	$6.53 \cdot 10^{-2}$	$2.08 \cdot 10^{-3}$	$3.04 \cdot 10^1$
4	2113	175 360	$3.26 \cdot 10^{-2}$	$5.21 \cdot 10^{-4}$	$6.26 \cdot 10^1$

TABLE 4. Test Case 2: data of mesh family  $\mathcal{M}_{2B}$ .

*Test Case 2.* In the second test case, we consider the family of meshes shown in Figure 3. At each mesh-refinement step, we increase the number of edges per element. We consider two families of meshes,  $\mathcal{M}_{2A}$  and  $\mathcal{M}_{2B}$ , which are characterized by a different growth rate of  $h_P/\hat{h}_P$ . The

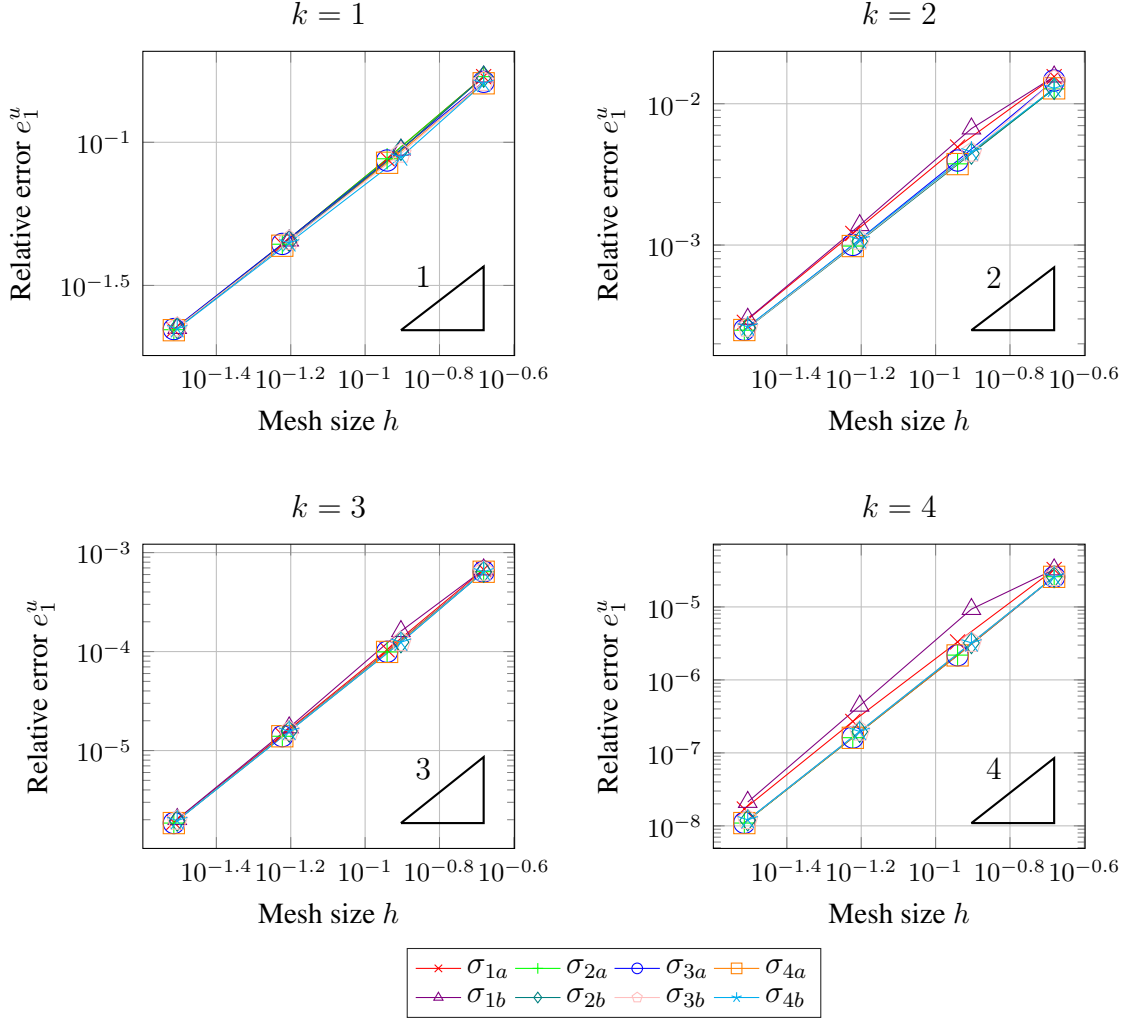


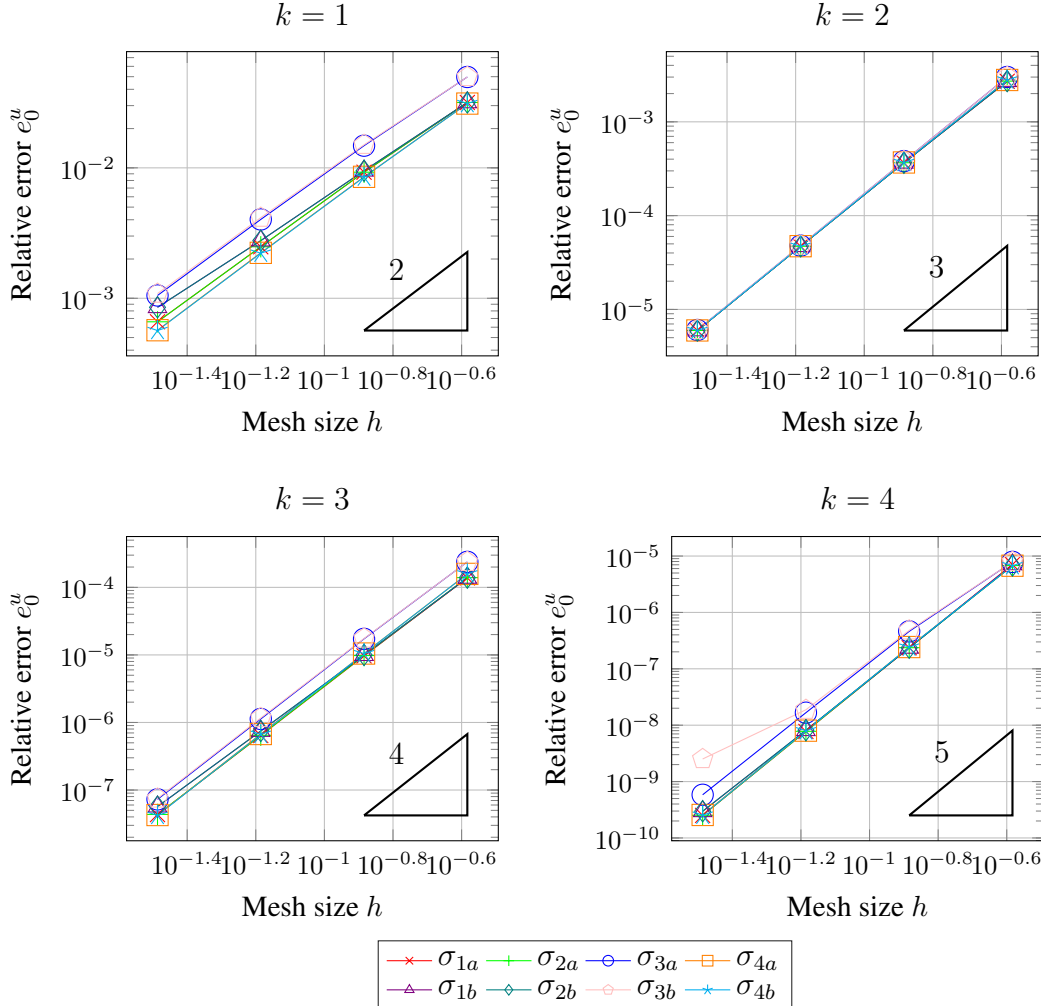
FIGURE 6. Test Case 1: convergence plots for  $e_1^u$  using the hexagonal meshes  $\mathcal{M}_{1A}$  and  $\mathcal{M}_{1B}$ , and the four stabilization strategies  $\sigma_i$ ,  $i = 1, 2, 3, 4$ . Top row: plots for  $k = 1$  (left panel) and  $k = 2$  (bottom panel); bottom row: plots for  $k = 3$  (left panel) and  $k = 4$  (right panel).

	1	14 (4)	16 (16)	20 (12)	24 (9)
2	20 (4)	24 (64)	30 (28)	40 (49)	
3	26 (4)	32 (256)	38 (60)	48 (225)	
4	34 (4)	40 (1024)	50 (124)	64 (961)	

TABLE 5. Test Case 2: additional data of mesh family  $\mathcal{M}_{2A}$ .

data of these meshes are collected in Tables 3-4. Additionally, for these meshes we report in Tables 5–6 the mesh number, the number of edges per element and for each one of these data, the number of elements having that specific number of edges. For example, the first line of Table 5, i.e., “1 14(4) 16(16) 20(12) 24(9)” must be read as: “*Mesh (refinement) 1 has 4 elements with 14 edges, 16 elements with 16 edges, 12 elements with 20 edges and 9 elements with 24 edges*”.

1	14 (4)	16 (16)	20 (12)	24 (9)
2	26 (4)	32 (64)	38 (28)	48 (49)
3	54 (4)	64 (256)	78 (60)	96 (225)
4	105 (4)	125 (1024)	155 (124)	195 (961)

TABLE 6. Test Case 2: additional data of mesh family  $\mathcal{M}_{2B}$ .FIGURE 7. Test Case 2: convergence plots for  $e_0^u$  using the polygonal meshes  $\mathcal{M}_{2A}$  and  $\mathcal{M}_{2B}$ , and the four stabilization strategies  $\sigma_i$ ,  $i = 1, 2, 3, 4$ . Top row: plots for  $k = 1$  (left panel) and  $k = 2$  (right panel); right row: plots for  $k = 3$  (left panel) and  $k = 4$  (bottom panel).

Figures 7 and 8 show the convergence plots of  $e_0^u$  and  $e_1^u$  that we obtain with the VEM and the stabilizations  $\sigma_i$ ,  $i = 1, 2, 3, 4$ .

As expected, the errors  $e_0^u$  and  $e_1^u$  behave like  $\mathcal{O}(h^{k+1})$  and  $\mathcal{O}(h^k)$ , respectively. However, we note that there is some loss of accuracy for  $k = 1, 3$  and  $4$  when we use the stabilizations  $\sigma_1$  and  $\sigma_2$ . On the other hand, the VEM with stabilizations  $\sigma_3$  and  $\sigma_4$  behaves similarly for  $k = 1, 2$  and  $3$  but

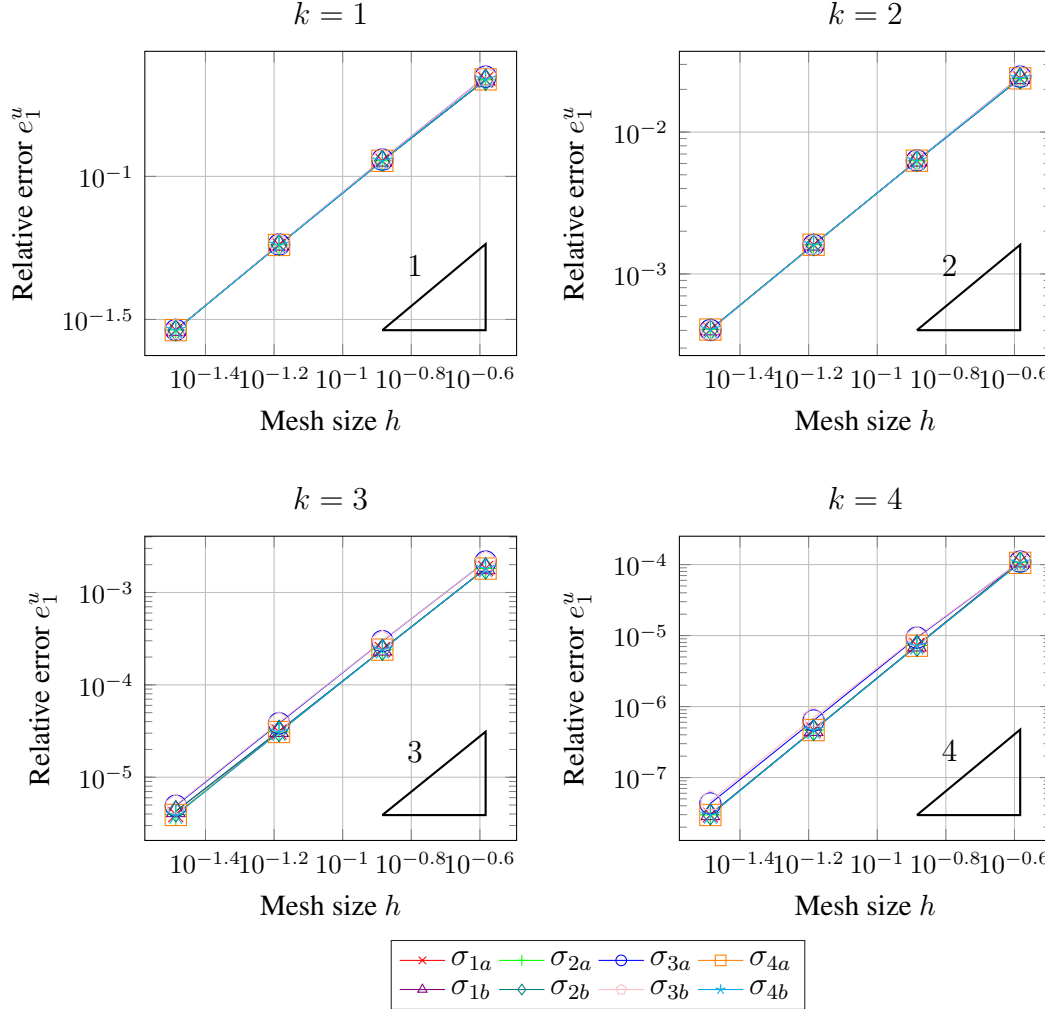


FIGURE 8. Test Case 2: convergence plots for  $e_1^u$  using the polygonal meshes  $\mathcal{M}_{2A}$  and  $\mathcal{M}_{2B}$ , and the four stabilization strategies  $\sigma_i$ ,  $i = 1, 2, 3, 4$ . Top row: plots for  $k = 1$  (left panel) and  $k = 2$  (bottom panel); bottom row: plots for  $k = 3$  (left panel) and  $k = 4$  (bottom panel).

Mesh	$N_{\text{el}}$	$N_{\text{ed}}$	$h$	$\hat{h}$	$\gamma_h$
1	64	576	$1.77 \cdot 10^{-1}$	$3.13 \cdot 10^{-2}$	5.66
2	256	4352	$8.84 \cdot 10^{-2}$	$7.81 \cdot 10^{-3}$	$1.13 \cdot 10^1$
3	1024	33 792	$4.42 \cdot 10^{-2}$	$1.95 \cdot 10^{-3}$	$2.26 \cdot 10^1$
4	4096	266 240	$2.21 \cdot 10^{-2}$	$4.88 \cdot 10^{-4}$	$4.53 \cdot 10^1$

TABLE 7. Test Case 3: data of mesh family  $\mathcal{M}_3$ .

for  $k = 4$ ,  $\sigma_3$  induces a visible loss in the convergence rate, possibly due to the effect of round-off. Instead, all versions of the VEM exhibit a similar behavior for  $e_1^u$ .

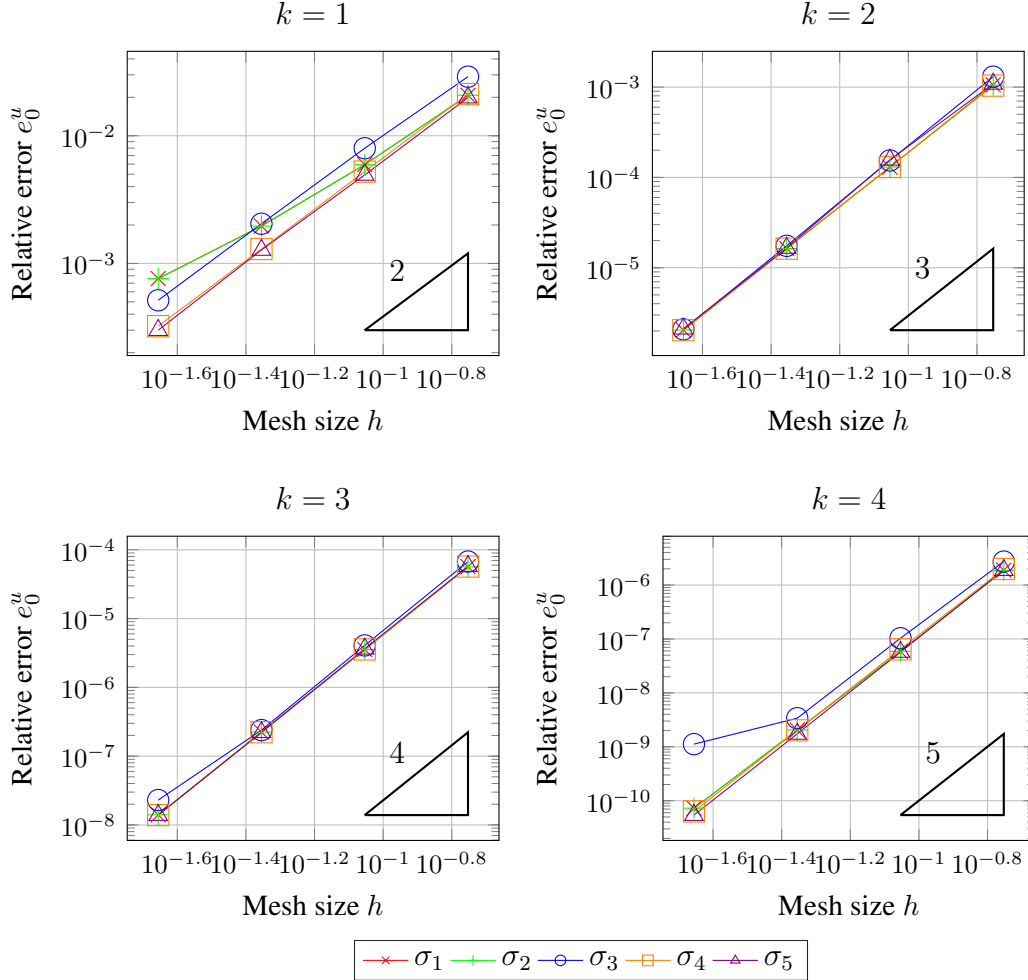


FIGURE 9. Test Case 3: convergence plots for  $e_0^u$  using the “squared” polygonal meshes  $\mathcal{M}_3$ , and the five stabilization strategies  $\sigma_i$ ,  $i = 1, 2, 3, 4, 5$ . Top row: plots for  $k = 1$  (left panel) and  $k = 2$  (bottom panel); bottom row: plots for  $k = 3$  (left panel) and  $k = 4$  (bottom panel).

*Test Case 3.* In the third test case, we consider the family of meshes shown in Figure 4. At each mesh refinement step, the number of edges per element is an increasing power of two, so that we can take the auxiliary grid  $\mathcal{G}_{\text{aux}}(\partial P)$  as the grid whose elements are the edges in  $\mathcal{E}_P$ . The data for these meshes are reported in Table 7.

Figures 9 and 10 show the convergence plots for  $e_0^u$  and  $e_1^u$  that we obtain with the stabilizations  $\sigma_i$ ,  $i = 1, 2, 3, 4, 5$ . We observe significative differences in the convergence rates for  $e_0^u$ . In particular, for  $k = 1$ , the stabilizations  $\sigma_1$  and  $\sigma_2$  perform poorly.

For  $k = 4$ , the performance of  $\sigma_3$  is extremely poor on the finest mesh. On the other hand, all the convergence plots for  $e_1^u$  show the optimal convergence rate proportional to  $\mathcal{O}(h^k)$  regardless of the stabilization.

The most robust stabilizations are  $\sigma_4$  and, when this is computed,  $\sigma_5$  (for technical reasons, depending on the wavelet implementation at our disposal, we only tested  $\sigma_5$  on the family  $\mathcal{M}_3$ ). However, the algorithm we used to compute the square-root of a matrix in  $\sigma_4$  (see [50]) failed to run in

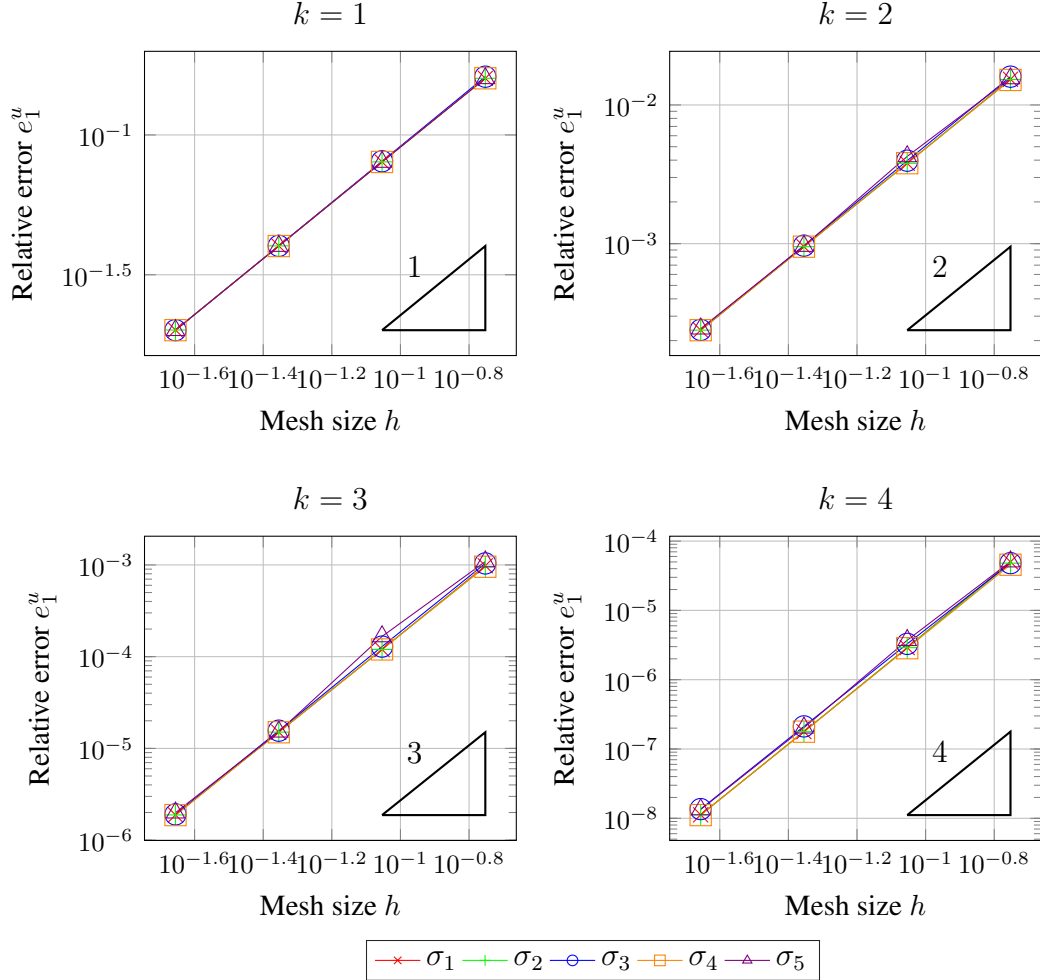


FIGURE 10. Test Case 3: convergence plots for  $e_1^u$  using the “squared” polygonal meshes  $\mathcal{M}_3$ , and the five stabilization strategies  $\sigma_i$ ,  $i = 1, 2, 3, 4, 5$ . Top row: plots for  $k = 1$  (left panel) and  $k = 2$  (bottom panel); bottom row: plots for  $k = 3$  (left panel) and  $k = 4$  (bottom panel).

some experiments on hexagonal meshes with more extreme values of the ratio  $h/\hat{h}$  than those of the  $\mathcal{M}_2$  family, due to round-off errors. More stable algorithms for computing the square-root of a matrix should be considered (see, for example, [44]).

## 7. CONCLUSIONS

We studied a novel approach to designing computable stabilizing bilinear forms for the nonconforming virtual element method, based on the duality technique first introduced in [20]. This consists in transferring the definition of the bilinear form from the local virtual element space to the dual space spanned by the functionals yielding the degrees of freedom. In such a way we could overcome the difficulty posed by the fact that, in the non conforming framework, the shape functions are non computable (not even as far as their trace on the boundary of the elements is concerned), and that the only information to which we have access along the computation are the values of the degrees

of freedom. By applying this novel technique, we built new bilinear forms with optimal or quasi-optimal stability bounds, under assumptions on the mesh which are weaker than the ones usually made in the analysis of the virtual element method, and which allow a mesh to have a very large number of arbitrarily small edges per element. The resulting discretization of second-order elliptic problems is accurate and robust, and allows for optimal or quasi-optimal error bounds. Finally, we numerically investigated the behavior of a non conforming VEM, implementing several examples of these new stabilization forms, and we assessed its performance on a set of representative test cases. The results of the numerical experiments confirmed the theoretical expectations.

### ACKNOWLEDGEMENTS

This paper has been realised in the framework of ERC Project CHANGE, which has received funding from the European Research Council (ERC) under the European Union’s Horizon 202 (grant agreement no. 694515), and of the project “Virtual Element Methods: Analysis and Applications”, funded by the MIUR Progetti di Ricerca di Rilevante Interesse Nazionale (PRIN) Bando 2017 (grant 201744KLJL).

### REFERENCES

- [1] R. A. Adams and J. J. F. Fournier. *Sobolev spaces*. Pure and Applied Mathematics. Academic Press, 2 edition, 2003.
- [2] B. Ahmad, A. Alsaedi, F. Brezzi, L. D. Marini, and A. Russo. Equivalent projectors for virtual element methods. *Comput. Math. Appl.*, 66:376–391, September 2013.
- [3] P. F. Antonietti, L. Beirão da Veiga, S. Scacchi, and M. Verani. A  $C^1$  virtual element method for the Cahn-Hilliard equation with polygonal meshes. *SIAM J. Numer. Anal.*, 54(1):34–56, 2016.
- [4] P. F. Antonietti, G. Manzini, and M. Verani. The fully nonconforming virtual element method for biharmonic problems. *Mathematical Models and Methods in Applied Sciences*, 28(02):387–407, 2018.
- [5] P. F. Antonietti, G. Manzini, and M. Verani. The conforming virtual element method for polyharmonic problems. *Comput. Math. Appl.*, 79(7):2021–2034, 2020.
- [6] P. F. Antonietti, L. Mascotto, and M. Verani. A multigrid algorithm for the  $p$ -version of the virtual element method. *ESAIM: Math. Model. Numer. Anal.*, 52(1):337–364, 2018.
- [7] B. Ayuso de Dios, K. Lipnikov, and G. Manzini. The non-conforming virtual element method. *ESAIM Math. Model. Numer.*, 50(3):879–904, 2016.
- [8] L. Beirão da Veiga, F. Brezzi, A. Cangiani, G. Manzini, L. D. Marini, and A. Russo. Basic principles of virtual element methods. *Math. Models Methods Appl. Sci.*, 23:119–214, 2013.
- [9] L. Beirão da Veiga, F. Brezzi, L. D. Marini, and A. Russo. Virtual element methods for general second order elliptic problems on polygonal meshes. *Math. Models Methods Appl. Sci.*, 26(4):729–750, 2016.
- [10] L. Beirão da Veiga, A. Chernov, L. Mascotto, and A. Russo. Basic principles of  $hp$  virtual elements on quasiuniform meshes. *Math. Models Methods Appl. Sci.*, 26(8):1567–1598, 2016.
- [11] L. Beirão da Veiga, K. Lipnikov, and G. Manzini. Arbitrary order nodal mimetic discretizations of elliptic problems on polygonal meshes. *SIAM J. Numer. Anal.*, 49(5):1737–1760, 2011.
- [12] L. Beirão da Veiga, K. Lipnikov, and G. Manzini. *The Mimetic Finite Difference Method*, volume 11 of *MS&A. Modeling, Simulations and Applications*. Springer, I edition, 2014.
- [13] L. Beirão da Veiga, C. Lovadina, and A. Russo. Stability analysis for the virtual element method. *Math. Models Methods Appl. Sci.*, 27(13):2557–2594, 2017.
- [14] L. Beirão da Veiga and G. Manzini. A virtual element method with arbitrary regularity. *IMA J. Numer. Anal.*, 34(2):782–799, 2014. DOI: 10.1093/imanum/drt018, (first published online 2013).
- [15] L. Beirão da Veiga and G. Manzini. Residual *a posteriori* error estimation for the virtual element method for elliptic problems. *ESAIM Math. Model. Numer. Anal.*, 49(2):577–599, 2015.
- [16] E. Benvenuti, A. Chiozzi, G. Manzini, and N. Sukumar. Extended virtual element method for the Laplace problem with singularities and discontinuities. *Comput. Methods Appl. Mech. Engrg.*, 356:571 – 597, 2019.

- [17] S. Berrone, A. Borio, and Manzini. SUPG stabilization for the nonconforming virtual element method for advection–diffusion–reaction equations. *Computer Methods in Applied Mechanics and Engineering*, 340:500–529, 2018.
- [18] S. Berrone, S. Pieraccini, S. Scialò, and F. Vicini. A parallel solver for large scale DFN flow simulations. *SIAM J. Sci. Comput.*, 37(3):C285–C306, 2015.
- [19] S. Bertoluzza. Substructuring preconditioners for the three fields domain decomposition method. *Math. Comp.*, 73(246):659–689, 2003.
- [20] S. Bertoluzza. Algebraic representation of dual scalar products and stabilization of saddle point problems. arXiv,1906.01296, 2019.
- [21] S. Bertoluzza, M. Pennacchio, and D. Prada. BDDC and FETI-DP for the virtual element method. *Calcolo*, 54:1565–1593, 2017.
- [22] S. Bertoluzza, M. Pennacchio, and D. Prada. FETI-DP for the three dimensional virtual element method. *SIAM Journal on Numerical Analysis*, 58(3):1556–1591, 2020.
- [23] S. Bertoluzza and D. Prada. A polygonal discontinuous Galerkin method with minus one stabilization. *ESAIM Math. Model. Numer.*, 2020.
- [24] P. E. Bjørstad and O. B. Widlund. Iterative methods for the solution of elliptic problems on regions partitioned into substructures. *SIAM J. Numer. Anal.*, 23(6):1093–1120, 1986.
- [25] F. Brackx, D. Constales, R. Ronveaux, and H. Serras. On the harmonic and monogenic decomposition of polynomials. *Journal of Symbolic Computation*, 8:297–304, 1989.
- [26] J. H. Bramble, J. E. Pasciak, and A. H. Schatz. The construction of preconditioners for elliptic problems by substructuring. I. *Math. Comp.*, 47(175):103–134, 1986.
- [27] S. C. Brenner. Poincaré–Friedrichs inequalities for piecewise  $H^1$  functions. *SIAM J. Numer. Anal.*, 41, 2003.
- [28] F. Brezzi. Stability of saddle-points in finite dimensions. In T. Shardlow J. F. Blowey, A. W. Craig, editor, *Frontiers in Numerical Analysis: Durham 2002*, Universitext, chapter 2. Springer, 2004.
- [29] F. Brezzi, A. Buffa, and K. Lipnikov. Mimetic finite differences for elliptic problems. *M2AN Math. Model. Numer. Anal.*, 43:277–295, 2009.
- [30] J. G. Calvo. An overlapping Schwarz method for virtual element discretizations in two dimensions. *Comput. Math. Appl.*, 77(4):1163–1177, 2019.
- [31] A. Cangiani, E. H. Georgoulis, T. Pryer, and O. J. Sutton. A posteriori error estimates for the virtual element method. *Numer. Math.*, 137:857–893, 2017.
- [32] A. Cangiani, V. Gyrya, and G. Manzini. The non-conforming virtual element method for the Stokes equations. *SIAM Journal on Numerical Analysis*, 54(6):3411–3435, 2016.
- [33] A. Cangiani, V. Gyrya, G. Manzini, and Sutton. O. Chapter 14: Virtual element methods for elliptic problems on polygonal meshes. In K. Hormann and N. Sukumar, editors, *Generalized Barycentric Coordinates in Computer Graphics and Computational Mechanics*, pages 1–20. CRC Press, Taylor & Francis Group, 2017.
- [34] A. Cangiani, G. Manzini, A. Russo, and N. Sukumar. Hourglass stabilization of the virtual element method. *Internat. J. Numer. Methods Engrg.*, 102(3-4):404–436, 2015.
- [35] A. Cangiani, G. Manzini, and O. Sutton. Conforming and nonconforming virtual element methods for elliptic problems. *IMA Journal on Numerical Analysis*, 37:1317–1354, 2017. (online August 2016).
- [36] S. Cao and L. Chen. Anisotropic error estimates of the linear nonconforming virtual element methods. *SIAM Journal on Numerical Analysis*, 57:1058–1081, 01 2019.
- [37] O. Certik, F. Gardini, G. Manzini, L. Mascotto, and G. Vacca. The p- and hp-versions of the virtual element method for elliptic eigenvalue problems. *Comput. Math. Appl.*, 79(7):2035–2056, 2020.
- [38] O. Certik, F. Gardini, G. Manzini, and G. Vacca. The virtual element method for eigenvalue problems with potential terms on polytopic meshes. *Applications of Mathematics*, 63(3):333–365, 2018.
- [39] A. Cohen, I. Daubechies, and J.-C. Feauveau. Biorthogonal bases of compactly supported wavelets. *Communications on Pure and Applied Mathematics*, 45(5):485–560, 1992.
- [40] W. Dahmen. Stability of multiscale transformations. *Journal of Fourier Analysis and Applications*, 2(4):341–361, 1996.
- [41] F. Dassi and L. Mascotto. Exploring high-order three dimensional virtual elements: bases and stabilizations. *Comput. Math. Appl.*, 75(9):3379–3401, 2018.
- [42] F. Dassi and S. Scacchi. Parallel block preconditioners for three-dimensional virtual element discretizations of saddle-point problems. *Computer Methods in Applied Mechanics and Engineering*, 372, 2020.

- [43] F. Dassi and S. Scacchi. Parallel solvers for virtual element discretizations of elliptic equations in mixed form. *Computers & Mathematics with Applications*, 79(7):1972–1989, 2020.
- [44] E. Deadman, N. J. Higham, and R. Ralha. Blocked Schur algorithms for computing the matrix square root. In Pekka Manninen and Per Öster, editors, *Applied Parallel and Scientific Computing*, pages 171–182, Berlin, Heidelberg, 2013. Springer Berlin Heidelberg.
- [45] D. A. Di Pietro, J. Droniou, and G. Manzini. Discontinuous skeletal gradient discretisation methods on polytopal meshes. *J. Comput. Phys.*, 355:397–425, 2018.
- [46] Antonietti P. F., S. Bertoluzza, D. Prada, and M. Verani. The virtual element method for a minimal surface problem. *Calcolo*, 57, 2020.
- [47] B. Faermann. Localization of the Aronszajn-Slobodeckij norm and application to adaptive boundary elements methods. Part I. The two-dimensional case. *IMA J. Numer. Anal.*, 20(2):203–234, 2000.
- [48] F. Gardini, G. Manzini, and G. Vacca. The nonconforming virtual element method for eigenvalue problems. *ESAIM: Mathematical Modelling and Numerical Analysis*, 53:749–774, 2019.
- [49] P. Hénon, P. Ramet, and J. Roman. PaStiX: a high-performance parallel direct solver for sparse symmetric positive definite systems. *Parallel Computing*, 28(2):301–321, 2002.
- [50] N. H. Higham. Computing real square roots of a real matrix. *Linear Algebra and its Applications*, 88–89:405–430, 1987.
- [51] J. Huang and Y. Yu. A medius error analysis for nonconforming virtual element methods for Poisson and biharmonic equations. *J. Comput. Appl. Math.*, 386, 04 2021.
- [52] M. Li, J. Zhao, C. Huang, and S. Chen. Nonconforming virtual element method for the time fractional reaction–subdiffusion equation with non-smooth data. *Journal of Scientific Computing*, 2019.
- [53] K. Lipnikov, G. Manzini, and M. Shashkov. Mimetic finite difference method. *J. Comput. Phys.*, 257 – Part B:1163–1227, 2014.
- [54] G. Manzini, K. Lipnikov, J. D. Moulton, and M. Shashkov. Convergence analysis of the mimetic finite difference method for elliptic problems with staggered discretizations of diffusion coefficients. *SIAM J. Numer. Anal.*, 55(6):2956–2981, 2017.
- [55] G. Manzini, A. Russo, and N. Sukumar. New perspectives on polygonal and polyhedral finite element methods. *Math. Models Methods Appl. Sci.*, 24(8):1621–1663, 2014.
- [56] L. Mascotto, I. Perugia, and A. Pichler. A nonconforming Trefftz virtual element method for the Helmholtz problem. *Mathematical Models and Methods in Applied Sciences*, 29, 08 2019.
- [57] L. Mascotto, I. Perugia, and A. Pichler. A nonconforming Trefftz virtual element method for the Helmholtz problem: Numerical aspects. *Computer Methods in Applied Mechanics and Engineering*, 347, 2019.
- [58] L. Mascotto and A. Pichler. Extension of the nonconforming Trefftz virtual element method to the Helmholtz problem with piecewise constant wave number. *Applied Numerical Mathematics*, 2019.
- [59] D. Mora, G. Rivera, and R. Rodríguez. A virtual element method for the Steklov eigenvalue problem. *Math. Methods Appl. Sci.*, 25(08):1421–1445, 2015.
- [60] G. H. Paulino and A. L. Gain. Bridging art and engineering using Escher-based virtual elements. *Struct. and Multidisciplinary Optim.*, 51(4):867–883, 2015.
- [61] I. Perugia, P. Pietra, and A. Russo. A plane wave virtual element method for the Helmholtz problem. *ESAIM Math. Model. Num.*, 50(3):783–808, 2016.
- [62] O. Steinbach. On a generalized  $L_2$  projection and some related stability estimates in Sobolev space s. *Numer. Math.*, 90:775–786, 2002.
- [63] P. Wriggers, W. T. Rust, and B. D. Reddy. A virtual element method for contact. *Comput. Mech.*, 58(6):1039–1050, 2016.
- [64] B. Zhang, J. Zhao, Y. Yang, and S. Chen. The nonconforming virtual element method for elasticity problems. *Journal of Computational Physics*, 378:394–410, 2019.
- [65] J. Zhang, B. andZhao and S. Chen. The nonconforming virtual element method for fourth-order singular perturbation problem. *Adv. Comput. Math.*, 46, 2020. (to appear).
- [66] J. Zhao, S. Chen, and B. Zhang. The nonconforming virtual element method for plate bending problems. *Mathematical Models & Methods in Applied Sciences*, 26(9):1671–1687, 2016.
- [67] J. Zhao, B. Zhang, S. Mao, and S. Chen. The divergence-free nonconforming virtual element method for the Stokes problem. *SIAM Journal on Numerical Analysis*, 57(6):2730–2759, 2019.

[68] J. Zhao, B. Zhang, S. Mao, and S. Chen. The nonconforming virtual element method for the Darcy-Stokes problem. *Computer Methods in Applied Mechanics and Engineering*, 370:113251–, 2020.

#### APPENDIX A. PROOF OF LEMMA 4.1

Let  $v \in V_k^h(P)$  and  $\hat{v} \in V_k^{h,\text{en}}(P)$  satisfy (39). We recall that such a condition implies that  $\Pi_k^{\nabla,P} v = \Pi_k^{\nabla,P} \hat{v}$ . As  $\Delta v \in \mathbb{P}_{k-2}(P)$  and  $(\nabla v \cdot \mathbf{n}_P)|_e \in \mathbb{P}_{k-1}(e)$  for all  $e \in \mathcal{E}_P$  we have

$$\begin{aligned} |v|_{1,P}^2 &= \int_P |\nabla v|^2 = - \int_P \Delta v v + \int_{\partial P} \nabla v \cdot \mathbf{n}_P v = - \int_P \Delta v \hat{v} + \int_{\partial P} \nabla v \cdot \mathbf{n}_P \hat{v} \\ &= \int_P \nabla v \cdot \nabla \hat{v} \leq |v|_{1,P} |\hat{v}|_{1,P}. \end{aligned}$$

We divide both sides by  $|v|_{1,P}$  and obtain the upper bound. On the other hand, we observe that, as  $\Delta(\hat{v} - \Pi_k^{\nabla,P} \hat{v}) \in \mathbb{P}_k$ , it can be split as

$$\Delta(\hat{v} - \Pi_k^{\nabla,P} \hat{v}) = D_1(\hat{v}) + D_2(\hat{v})$$

with  $D_1(\hat{v}) \in \mathbb{P}_{k-2}(P)$  and  $D_2(\hat{v})$  belonging to the linear space spanned by  $\mathcal{M}_k(P) \setminus \mathcal{M}_{k-2}(P)$ , and that we have

$$\|\Delta(\hat{v} - \Pi_k^{\nabla,P} \hat{v})\|_{0,P} \simeq \|D_1(\hat{v})\|_{0,P} + \|D_2(\hat{v})\|_{0,P}.$$

We observe that, in view of the definition of the enhanced space, we have that

$$\int_P D_2(\hat{v})(\hat{v} - \Pi_k^{\nabla,P} \hat{v}) = \int_P D_2(\hat{v})(\Pi_k^{\nabla,P} \hat{v} - \Pi_k^{\nabla,P} \hat{v}) = 0.$$

Then we can write:

$$\begin{aligned} \int_P |\nabla(\hat{v} - \Pi_k^{\nabla,P} \hat{v})|^2 &= - \int_P \Delta(\hat{v} - \Pi_k^{\nabla,P} \hat{v})(\hat{v} - \Pi_k^{\nabla,P} \hat{v}) + \int_{\partial P} \nabla(\hat{v} - \Pi_k^{\nabla,P} \hat{v}) \cdot \mathbf{n}_P (\hat{v} - \Pi_k^{\nabla,P} \hat{v}) = \\ &= - \int_P D_1(\hat{v})(\hat{v} - \Pi_k^{\nabla,P} \hat{v}) + \int_{\partial P} \nabla(\hat{v} - \Pi_k^{\nabla,P} \hat{v}) \cdot \mathbf{n}_P (v - \Pi_k^{\nabla,P} v) \\ &= - \int_P D_1(\hat{v})(v - \Pi_k^{\nabla,P} v) + \int_P \Delta(\hat{v} - \Pi_k^{\nabla,P} \hat{v})(v - \Pi_k^{\nabla,P} v) \\ &\quad + \int_P \nabla(\hat{v} - \Pi_k^{\nabla,P} \hat{v}) \cdot \nabla(v - \Pi_k^{\nabla,P} v). \end{aligned}$$

Then we have

$$\int_P |\nabla(\hat{v} - \Pi_k^{\nabla,P} \hat{v})|^2 \lesssim \|\Delta(\hat{v} - \Pi_k^{\nabla,P} \hat{v})\|_{0,P} \|v - \Pi_k^{\nabla,P} v\|_{0,P} + |\hat{v} - \Pi_k^{\nabla,P} \hat{v}|_{1,P} |v - \Pi_k^{\nabla,P} v|_{1,P}$$

Using Lemma 4.4 and a Poincaré inequality finally yields

$$\int_P |\nabla(\hat{v} - \Pi_k^{\nabla,P} \hat{v})|^2 \lesssim |\hat{v} - \Pi_k^{\nabla,P} \hat{v}|_{1,P} |v - \Pi_k^{\nabla,P} v|_{1,P}.$$

Dividing both sides by  $|\hat{v} - \Pi_k^{\nabla,P} \hat{v}|_{1,P}$  and using a triangular inequality yields the lower bound.

## APPENDIX B. PROOF OF LEMMA 4.6

Let  $\eta \in N_{k-1}(\partial P)$  with  $\int_{\partial P} \eta = 0$ . Let  $\mathbb{P}_{k+1}^0(e) = \mathbb{P}_{k+1}(e) \cap H_0^1(e)$  and observe that

$$\inf_{\eta \in \mathbb{P}_{k-1}(e)} \sup_{q \in \mathbb{P}_{k+1}^0(e)} \frac{\int_e \eta q}{\|\eta\|_{0,e} \|q\|_{0,e}} \gtrsim 1. \quad (66)$$

Relation (66) can be proven on the reference interval  $\hat{e} = [0, 1]$  by noting that the Riesz isomorphism between  $H^{-1}(e)$  and  $H_0^1(e)$  maps  $\mathbb{P}_{k-1}(\hat{e})$  to  $\mathbb{P}_{k+1}^0(\hat{e})$ , and that all norms are the equivalent on such finite dimensional spaces. Then, we apply a scaling argument to obtain (66) for a generic edge  $e$ . This implies that for every edge  $e \in \mathcal{E}_P$ , a function  $\phi_e(\eta) \in \mathbb{P}_{k+1}^0(e)$  exists such that

$$\|\eta\|_{0,e}^2 = \int_e \eta \phi_e(\eta), \quad \|\phi_e(\eta)\|_{0,e} \simeq \|\eta\|_{0,e}.$$

We let  $\phi \in H^{\frac{1}{2}}(\partial P)$  denote the function satisfying  $\phi|_e = h_e \phi_e(\eta)$  for all  $e \in \mathcal{E}_P$ , and we write

$$\sum_e h_e \|\eta\|_{0,e}^2 \leq \sum_e h_e \int_e \eta \phi_e(\eta) = \int_{\partial P} \eta \phi. \quad (67)$$

As  $\int_{\partial P} \eta = 0$ , for  $\bar{\phi} = \int_{\partial P} \phi$  we can write

$$\int_{\partial P} \eta \phi = \int_{\partial P} \eta (\phi - \bar{\phi}) \lesssim |\eta|_{-1/2,\partial P} |\phi - \bar{\phi}|_{1/2,\partial P} = |\eta|_{-1/2,\partial P} |\phi|_{1/2,\partial P}. \quad (68)$$

It remains to bound  $|\phi|_{1/2,\partial P}$ . First, we split  $\phi$  as  $\phi = \phi_1 + \phi_2$  where  $\phi_1$  is supported on the edges of  $\mathcal{E}_P^1$  and  $\phi_2$  on the edges of  $\mathcal{E}_P^2$ . Let  $\hat{\phi}_e$  denote the pullback of  $\phi_e$  on the reference edge  $\hat{e} = [0, 1]$ . We use again a scaling argument and the equivalence of all norms on the finite dimensional space  $\mathbb{P}_{k+1}^0(\hat{e})$  to find that

$$\begin{aligned} |\phi_2|_{1/2,\partial P} &\lesssim \sum_{e \in \mathcal{E}_P^2} \|h_e \phi_e(\eta)\|_{H_{00}^{\frac{1}{2}}(e)} = \sum_{e \in \mathcal{E}_P^2} h_e \|\hat{\phi}_e\|_{H_{00}^{\frac{1}{2}}(\hat{e})} \lesssim \sum_{e \in \mathcal{E}_P^2} h_e \|\hat{\phi}_e\|_{0,\hat{e}} \\ &= \sum_{e \in \mathcal{E}_P^2} h_e^{1/2} \|\phi_e(\eta)\|_{0,e} \lesssim \sqrt{N^*} \left( \sum_{e \in \mathcal{E}_P^2} h_e \|\phi_e(\eta)\|_{0,e}^2 \right)^{1/2} \leq \sqrt{N^*} \left( \sum_{e \in \mathcal{E}_P^2} h_e \|\eta\|_{0,e}^2 \right)^{1/2}, \end{aligned}$$

where we recall that, for an edge  $e \in \mathcal{E}_P$ , the space  $H_{00}^{\frac{1}{2}}(e)$  is the space of functions  $\eta$  in  $H^{\frac{1}{2}}(e)$  such that the function  $E\eta \in L^2(\partial P)$  satisfying  $E\eta|_e = \eta$  and  $E\eta|_{\partial P \setminus e} = 0$  is in  $H^{\frac{1}{2}}(\partial P)$ , endowed with the norm  $\|\eta\|_{H_{00}^{\frac{1}{2}}(e)} = |E\eta|_{1/2,\partial P}$ .

To bound  $|\phi_1|_{1/2,\partial P}$ , we proceed as in [47], taking advantage that the grid is locally quasi uniform on the support of  $\phi_1$ . Let  $\omega_e$  denote the patch given by the union of  $e \in \mathcal{E}_P$  and its two neighboring edges. Then, we have that

$$|\phi_1|_{1/2,\partial P}^2 = \sum_{e \in \mathcal{E}_P} \int_e \left[ \int_{\omega_e} \frac{|\phi_1(x) - \phi_1(y)|^2}{|x - y|^2} dx dy + \int_{\partial P \setminus \omega_e} \frac{|\phi_1(x) - \phi_1(y)|^2}{|x - y|^2} dx dy \right]. \quad (69)$$

With our definition of  $\mathcal{E}_P^1$  and  $\phi_1$ , we see that

$$\sum_{e \in \mathcal{E}_P} \int_e \int_{\omega_e} \frac{|\phi_1(x) - \phi_1(y)|^2}{|x - y|^2} dx dy \lesssim \sum_{e \in \mathcal{E}_P^1} \int_{\omega_e} \int_{\omega_e} \frac{|\phi_1(x) - \phi_1(y)|^2}{|x - y|^2} dx dy = \sum_{e \in \mathcal{E}_P^1} |\phi_1|_{1/2,\omega_e}^2.$$

Assumption **(G3.1)** allows us to use an inverse inequality on  $\omega_e$ , which yields

$$\sum_{e \in \mathcal{E}_P^1} |\phi_1|_{1/2, \omega_e}^2 \lesssim \sum_{e \in \mathcal{E}_P^1} \sum_{e' \subset \omega_e} h_{e'}^{-1} \|\phi_1\|_{0, e'}^2 = \sum_{e \in \mathcal{E}_P^1} h_e \|\eta\|_{0, e}^2.$$

On the other hand, we can write

$$\begin{aligned} & \sum_{e \in \mathcal{E}_P} \int_e \int_{\partial P \setminus \omega_e} \frac{|\phi_1(x) - \phi_1(y)|^2}{|x - y|^2} dx dy \\ & \lesssim \sum_{e \in \mathcal{E}_P} \int_e \int_{\partial P \setminus \omega_e} \frac{|\phi_1(x)|^2}{|x - y|^2} dx dy + \sum_{e \in \mathcal{E}_P} \int_e \int_{\partial P \setminus \omega_e} \frac{|\phi_1(y)|^2}{|x - y|^2} dx dy \\ & = 2 \sum_{e \in \mathcal{E}_P^1} \int_e |\phi_1(x)|^2 \left( \int_{\partial P \setminus \omega_e} \frac{1}{|x - y|^2} dy \right) dx, \end{aligned}$$

where the second term of the sum in the second step can be seen to be equal to first one by splitting the integral in  $y$  over the union of edges in  $\mathcal{E}_P^1 \setminus \omega_e$  and switching the two integrals. By direct calculation, under our assumptions, we find the bound

$$\int_{\partial P \setminus \omega_e} \frac{1}{|x - y|^2} dy \lesssim h_e^{-1},$$

finally yielding

$$\sum_{e \in \mathcal{E}_P} \int_e \int_{\partial P \setminus \omega_e} \frac{|\phi_1(x) - \phi_1(y)|^2}{|x - y|^2} dx dy \lesssim \sum_{e \in \mathcal{E}_P^1} h_e^{-1} \|\phi_1\|_{0, e}^2 \lesssim \sum_{e \in \mathcal{E}_P^1} h_e \|\eta\|_{0, e}^2.$$

Collecting the contributions of  $\phi_1$  and  $\phi_2$  we finally have that

$$|\phi|_{1/2, \partial P}^2 \lesssim \sum_{e \in \mathcal{E}_P} h_e \|\eta\|_{0, e}^2.$$

Substituting such a bound in (68) and using the result in (67) we then write

$$\sum_e h_e \|\eta\|_{0, e}^2 = \int_{\partial P} \eta \phi \lesssim |\eta|_{-1/2, \partial P} \left( \sum_e h_e \|\eta\|_{0, e}^2 \right)^{1/2},$$

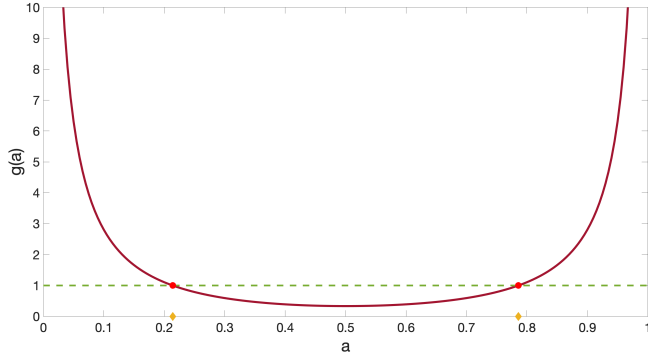
and dividing both sides by the square root of  $\sum_e h_e \|\eta\|_{0, e}^2$  yields

$$|\eta|_{-1/2, \partial P} \gtrsim \left( \sum_e h_e \|\eta\|_{0, e}^2 \right)^{1/2},$$

which concludes the proof.

## APPENDIX C. THE STEINBACH PROJECTOR

In this section we review a result by O. Steinbach [62] on the boundedness in  $H^s$  of the projector onto the space of continuous piecewise linears, orthogonally to the space of piecewise constants on the dual grid, which we adapt to the case at hand by switching the roles of the two grids. By a scaling argument it is sufficient to consider the case  $|\partial P| = 1$ . Let  $\mathcal{G} = \{e_k, k = 1, \dots, M\}$  denote a decomposition of  $\partial P$  and let  $\hat{h}_k = |e_k|$ . Let  $x_k$  denote the midpoint of the interval  $e_k$  and

FIGURE 11. The function  $g(a)$  for which  $\lambda(a) = 1 \pm g(a)$ 

$\mathcal{G}^* = \{\tau_\ell, \ell = 1, \dots, M\}$ , with  $\tau_\ell = [x_\ell, x_{\ell+1}]$ , the dual grid, with the ‘‘cyclic’’ convention that  $x_{M+1} = x_1, e_{M+1} = e_1$ . We let  $h_\ell = |\tau_\ell|$  denote the length of  $\tau_\ell$ .

We make the assumption that  $\mathcal{G}$  is locally quasi uniform, that is, that there exists  $c' \geq 1$  such that for all  $k$  it holds that

$$\frac{1}{c'} \leq \frac{\hat{h}_k}{\hat{h}_{k+1}} \leq c'. \quad (70)$$

We let  $\tilde{K}(\mathcal{G}^*) = \text{span}\{\phi_k\}_{k=1}^M \subset H^1(\partial P)$  and  $K(\mathcal{G}) = \text{span}\{\psi_k\}_{k=1}^M \subset L^2(\partial P)$  denote, respectively, the space of continuous piecewise linears on the grid  $\mathcal{G}^*$  and the space of piecewise constants on the grid  $\mathcal{G}$ . Here,  $\phi_k$  is the nodal basis function corresponding to  $x_k$  and  $\psi_k$  is the characteristic function of the interval  $e_k$ . Observe that the dual grid  $\mathcal{G}^*$  is itself locally quasi uniform. Moreover, the local mesh sizes are comparable, that is, there exist a positive constant  $c$  such that, for  $\ell, k$  with  $\tau_\ell \cap e_k \neq \emptyset$

$$\frac{1}{c} \leq \frac{\hat{h}_k}{h_\ell} \leq c. \quad (71)$$

We let  $\tilde{Q} : L^2(\partial P) \rightarrow \tilde{K}(\mathcal{G}^*)$  denote the projection operator defined as the solution to the variational problem

$$\int_{\partial P} \tilde{Q}uw = \int_{\partial P} uw, \quad \forall w \in K(\mathcal{G}).$$

With the same proof as in [62], we find that the operator  $\tilde{Q}$  is well defined and bounded in  $L^2(\partial P)$  with a constant that does not depend on the size and number of the elements but only on the constant  $c'$  in (70). Let the local Gramian matrix be defined by

$$\tilde{\mathbb{G}}_\ell^*[i, j] = \int_{\tau_\ell} \psi_{\ell+i-1} \phi_{\ell+j-1}, \quad 1 \leq i, j \leq 2.$$

Moreover, let  $D_\ell$  and  $H_\ell$  be the diagonal matrices defined by

$$(D_\ell)_{i,i} = (\tilde{\mathbb{G}}_\ell^*)_{i,i}, \quad (H_\ell)_{i,i} = \hat{h}_{\ell+i-1}^s, \quad 1 \leq i \leq 2.$$

Then, we find that the results stated in the following theorem holds. The proof is the same of the analogous results in [62], though in such a paper the roles of the two grids are switched (the space

of piecewise constants is definded on  $\mathcal{G}^*$  and the space of continuous piecewise linears on  $\mathcal{G}$ ), and it hence is omitted.

**Theorem C.1.** *Assume that there exists a positive constant  $\alpha_0$  such that*

$$\mathbf{x}^T \mathbf{H}_\ell \tilde{\mathbf{G}}_\ell^* \mathbf{H}_\ell^{-1} \mathbf{x} \geq \alpha_0 \mathbf{x}^T \mathbf{D}_\ell \mathbf{x} \quad (72)$$

for all  $\mathbf{x} \in \mathbb{R}^2$  and any integer  $\ell = 1, \dots, M$ . Then,  $\tilde{Q}$  is bounded in  $H^s(\partial P)$  by a constant not depending on the size and number of the elements.

It is now possible to give an explicit sufficient condition on the constant  $c'$  in (70), in order for (72) to hold for some positive constant  $\alpha_0$ . Indeed, let us focus on an element  $\tau_\ell$  whose vertices are the mid points of two adjacent elements  $e_1$  and  $e_2$  of length  $\hat{h}_1$  and  $\hat{h}_2$ . We have  $h_\ell = (\hat{h}_1 + \hat{h}_2)/2$ . Let us rescale everything in such a way that

$$h_\ell = 1, \quad \hat{h}_1 = 2a, \quad \hat{h}_2 = 2(1-a), \quad \text{with } a \in (0, 1).$$

A direct computation yields

$$\tilde{\mathbf{G}}_\ell^* = \frac{1}{2} \begin{pmatrix} (2-a)a & a^2 \\ (1-a)^2 & 1-a^2 \end{pmatrix}.$$

We can rewrite condition (72) in simmetric form as

$$\mathbf{y}^T \mathbf{M}_\ell \mathbf{y} \geq \alpha_0 \mathbf{y}^T \mathbf{y}, \quad \mathbf{M}_\ell = \frac{1}{2} \mathbf{D}_\ell^{-1/2} \left( \mathbf{H}_\ell \tilde{\mathbf{G}}_\ell^* \mathbf{H}_\ell^{-1} + \mathbf{H}_\ell^{-1} (\tilde{\mathbf{G}}_\ell^*)^T \mathbf{H}_\ell \right) \mathbf{D}_\ell^{-1/2}. \quad (73)$$

A constant  $\alpha_0 > 0$  exists such that (72) holds for all  $\mathbf{y} \in \mathbb{R}^2$  if and only if  $\mathbf{M}_\ell$  is a positive definite matrix, and  $\alpha_0$  is then its lowest eigenvalue. Considering the case  $s = 1/2$ , a direct computation yields the following eigenvalues for  $\mathbf{M}_\ell$

$$\lambda = 1 \pm \frac{1}{2} \frac{\sqrt{a+1}(3a^2 - 3a + 1)}{\sqrt{2-a}(a - a^3)} = 1 \pm g(a) \quad (74)$$

where  $g(a)$  is non negative for  $a \in (0, 1)$ , see Figure 11.

The lowest eigenvalue stems then from the minus sign in (74), and it is positive if  $g(a) < 1$ . We solve such an inequality numerically and obtain that  $a$  must satisfy  $a_0 < a < 1 - a_0$  with  $a_0 \sim 0.214009576006805$  for condition (72) to be true. Now, we translate such condition on  $a$  on a condition on the constant  $c'$  appearing in equation (70). More precisely, condition (72) is satisfied if the inequalities in (70) hold with  $c' < (1 - a_0)/a_0 \sim 3.672688104237926$ . The optimal value for  $\alpha_0$  is attained when  $a = 1/2$ , which corresponds to  $c' = 1$ , e.g., the uniform grid case. In such a case, the smallest eigenvalue of  $M_\ell$  is  $\lambda = 2/3$ .